

Role of Ester Sulfate and Organic Disulfide in Mercury Methylation in Peatland Soils

Caroline E. Pierce, Olha S. Furman, Sarah L. Nicholas, Jill Coleman Wasik, Caitlin M. Gionfriddo, Ann M. Wymore, Stephen D. Sebestyen, Randall K. Kolka, Carl P. J. Mitchell, Natalie A. Griffiths, Dwayne A. Elias, Edward A. Nater, and Brandy M. Toner*



Cite This: *Environ. Sci. Technol.* 2022, 56, 1433–1444



Read Online

ACCESS |



Metrics & More



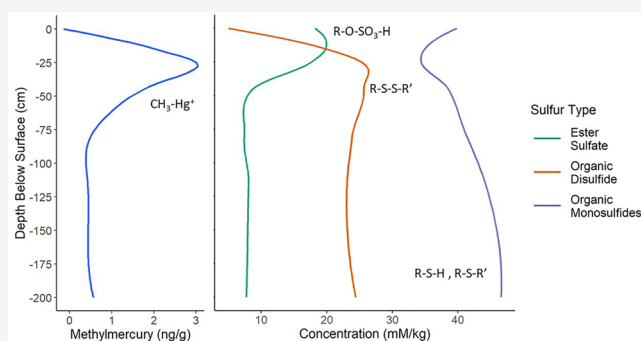
Article Recommendations



Supporting Information

ABSTRACT: We examined the composition and spatial correlation of sulfur and mercury pools in peatland soil profiles by measuring sulfur speciation by 1s X-ray absorption near-edge structure spectroscopy and mercury concentrations by cold vapor atomic fluorescence spectroscopy. Also investigated were the methylation/demethylation rate constants and the presence of *hgcAB* genes with depth. Methylmercury (MeHg) concentration and organic disulfide were spatially correlated and had a significant positive correlation ($p < 0.05$). This finding is consistent with these species being products of dissimilatory sulfate reduction. Conversely, a significant negative correlation between organic monosulfides and MeHg was observed, which is consistent with a reduction in Hg(II) bioavailability via complexation reactions. Finally, a significant positive correlation between ester sulfate and instantaneous methylation rate constants was observed, which is consistent with ester sulfate being a substrate for mercury methylation via dissimilatory sulfate reduction. Our findings point to the importance of organic sulfur species in mercury methylation processes, as substrates and products, as well as potential inhibitors of Hg(II) bioavailability. For a peatland system with sub- $\mu\text{mol L}^{-1}$ porewater concentrations of sulfate and hydrogen sulfide, our findings indicate that the solid-phase sulfur pools, which have a much larger sulfur concentration range, may be accessible to microbial activity or exchanging with the porewater.

KEYWORDS: sulfur XANES, methylmercury, peatland



1. INTRODUCTION

Globally, boreal peatlands cover a land area of 4 million km², primarily in Russia, Canada, and the USA.¹ Within Minnesota, boreal peatlands cover a land area of 24,000 km².² Boreal peatlands are hot spots for the production of methylmercury (MeHg) that lead to toxic and environmentally detrimental levels.^{3–5} Methylmercury released from peatlands to aquatic systems can be biomagnified in the food web to top predatory fish that humans and wildlife consume.⁶ While sulfate-reducing bacteria (SRB) are considered to be important producers of MeHg, not all SRB methylate mercury.⁷ Cause and effect studies in peatlands demonstrate that the enhanced availability of sulfate leads to increased MeHg concentrations but the detailed information of how sulfur is transformed in organic soils remains unknown.^{8,9} Methanogens and some iron-reducing bacteria (IRB) also produce MeHg within boreal peatlands.^{10–12} However, the role of methanogens and IRB in mercury methylation is outside the scope of this article. We explore the interactions of sulfur and mercury via microbial sulfate reduction within a boreal peatland. It is unknown why microbes methylate mercury though there are hypotheses such

as detoxification of the cell, carbon metabolism, and metal homeostasis.^{13,14}

Biogeochemically linked elements, sulfur and mercury, enter ombrotrophic bogs (see Section 2.1) through atmospheric deposition and are cycled in the soil profile by physical, chemical, and biological processes. Cycling is especially active at depths where distinct contrasts in physical and chemical properties, such as water content and oxidation–reduction conditions occur.^{15–18} As an example of a chemical process, mercury has a high binding affinity for reduced organic sulfur (e.g., thiols).^{19–21} As an example of a biological process, dissimilatory SRB populations catalyze the reduction of sulfur and mercury methylation in peatland soils.^{8,9,22,23} Although

Received: July 14, 2021

Revised: November 16, 2021

Accepted: November 17, 2021

Published: January 3, 2022



porewater sulfate pools are small, oxidation reactions during periods of lowered water tables may recycle oxidized organic sulfur that can sustain sulfate reduction rates and net MeHg production following wetting events.^{17,24,25} Studies in low-sulfate environments demonstrate that organic sulfur compounds can be an important component of dissimilatory sulfate reduction.²⁶ Genomic studies have shown that some SRB are capable of utilizing ester sulfate.²⁷ However, this pathway has not been demonstrated in SRB that also methylate mercury. The functional genes that encode for mercury methylation in anaerobic microorganisms have been identified as *hgcAB*.^{10,28} We are not aware of any existing literature regarding the depth distribution of *hgcAB* genes within boreal peat.

In this study, we measured the abundance and speciation of mercury and sulfur, rates of methylation and demethylation, and the presence of *hgcAB* genes in peat profiles. Most lab and field studies to date have focused on inorganic sulfate as a driver for mercury methylation,^{8,18,21,29} but bogs have little inorganic sulfur.^{15,30} Our objective was to investigate the role of organic sulfur species, as opposed to inorganic sulfur species, in peatland soil as important reactants and products in mercury methylation. In a climate with an increasingly variable water table (i.e., longer drought with deeper water table position) a greater volume of peat may be exposed to biogeochemical processes that are able to generate ester sulfate and MeHg.^{15,31–36}

2. MATERIALS AND METHODS

2.1. Site Description. The field site, the S1 bog, is an ombrotrophic bog with a black spruce (*Picea mariana*) and tamarack (*Larix laricina*) overstory, located at the United States Department of Agriculture (USDA) Forest Service Marcell Experimental Forest (MEF) in northern Minnesota (47°30.476' N; 93°27.1620' W and 412 mamsl, Figure S1: map of the MEF). Bogs do not have inflow from groundwater and receive inputs only from the atmosphere, creating a mineral-poor ombrotrophic peatland.^{37,38} Mean annual air temperature at the MEF from 1961 to 2019 was 3.5 °C and average annual precipitation was 770 mm.³⁹ Much of the peat is 2–4 m deep and the peatland water table fluctuates seasonally within the upper 30 cm of peat during most years.^{40,41}

Water flows laterally through a shallow acrotelm and mesotelm to the peatland margin and to an outlet stream when the water table is high.⁴² The acrotelm is a surficial layer of low density and comparatively high hydraulic conductivity. It is mostly oxic above the water table and includes living plants and the majority of roots.⁴³ The catotelm is a deeper zone of permanently saturated and higher density peat with lower hydraulic conductivity and permanently anoxic conditions.^{44,45} Between the acrotelm and catotelm is the mesotelm (approximately 30–50 cm below the surface), a transitional area characterized by a fluctuating water table.^{35,40,45,46} The mesotelm is periodically oxic, corresponding to low water tables, or anoxic, corresponding to high water tables.

The S1 bog surface consists of raised hummocks alternating with microtopographical lows called hollows. All depths are measured relative to the hollow surface. Typical relief is 20–30 cm from hummock tops to adjacent hollows and the lateral extent of hummocks can be up to several meters wide.^{47,48} The bryophytes in hummocks consist mainly of *Sphagnum divinum* (previously *Sphagnum magellanicum*⁴⁹), while hollows are

mainly colonized by *Sphagnum angustifolium* and *Sphagnum fallax*. *S. angustifolium* and *S. fallax* have few readily distinguishable features, so we refer to them as *S. angustifolium/fallax*. The S1 bog is the site of the long-term and large-scale Spruce and Peatland Responses Under Changing Environments (SPRUCE) experiment where air and peat temperatures (0–+9 °C above ambient) and atmospheric carbon dioxide (CO₂) levels (ambient and +500 ppm) are being manipulated to study climate effects on ecological, hydrological, and biogeochemical processes in peatlands.⁵⁰ All data presented in this paper were collected prior to the onset of the experimental warming and elevated CO₂ treatments.

2.2. Sampling Methods. Peat cores were collected to a depth of –200 cm from six locations in triplicate for a total of 18 cores in August 2012.⁴⁷ See the Supporting Information for detailed coring, sampling intervals, and sampling methods. Samples for mercury were frozen and samples for sulfur were stored in argon and frozen. Living *S. divinum* and *S. angustifolium/fallax* were sampled in June 2014 and stored frozen before further analyses. Porewaters were collected from piezometers in 2013.⁵¹

The different sample types were collected in different years but all were collected from the same peat bog in late summer and early fall seasons. Peat soil was collected in August 2012, porewaters were collected in September 2013, and peat for the rate study was collected in 2016. Environmental conditions (water table height, temperature) were different between sampling time points. However, over the monitoring history of the MEF (since 1960), these factors have consistent seasonal ranges and all samples were collected in the same season although different years.

2.3. Sulfur Concentration and Speciation in Peatland Soil. Peat and *Sphagnum* samples were dried in a N₂ (g)-filled flow-through desiccator. The samples were then homogenized in a N₂ (g)-filled glovebag using a ceramic mortar and pestle and liquid nitrogen. Homogenized samples were stored in N₂ (g)-filled packs until analysis.

Total sulfur concentrations of dried and ground subsamples were measured by combustion using a carbon, nitrogen, sulfur Elementar Vario EL analyzer (Elementar Instruments).

Sulfur X-ray absorption near edge structure (XANES) data were acquired on beamlines 06B1-1 Soft X-ray Micro-characterization Beamline (SXRMB) at the Canadian Light Source (CLS, Saskatoon, SK, Canada) and 9-BM X-ray beamline at the Advanced Photon Source (APS, Argonne National Laboratory, Argonne, IL, USA). See the Supporting Information for detailed methods. Sulfur XANES spectra were processed using *Athena*.⁵² Linear combination fitting of the sample spectra with reference spectra was performed using *mrfit*.⁵³ We used a subset of a published sulfur reference database^{54–58} (Table S1: list of sulfur reference compounds).

2.4. Acid Volatile Sulfur and Sulfate in Porewaters. Porewaters were analyzed for sulfide concentration by protonating all acid-extractable sulfides to H₂S (g) and using the methylene blue colorimetric method.⁵⁹ The working range for this method was 0.01–2.0 mg L⁻¹.

Porewaters were analyzed for sulfate on a Thermo Dionex ICS-2100 ion chromatograph according to Standard Method 4110 C.^{51,60} The limit of detection was 0.02 mg L⁻¹ SO₄²⁻.

2.5. Total Mercury and MeHg Concentration in Peatland Soil. Total mercury (THg) was measured by cold vapor atomic fluorescence spectroscopy (CVAFS) on a Tekran

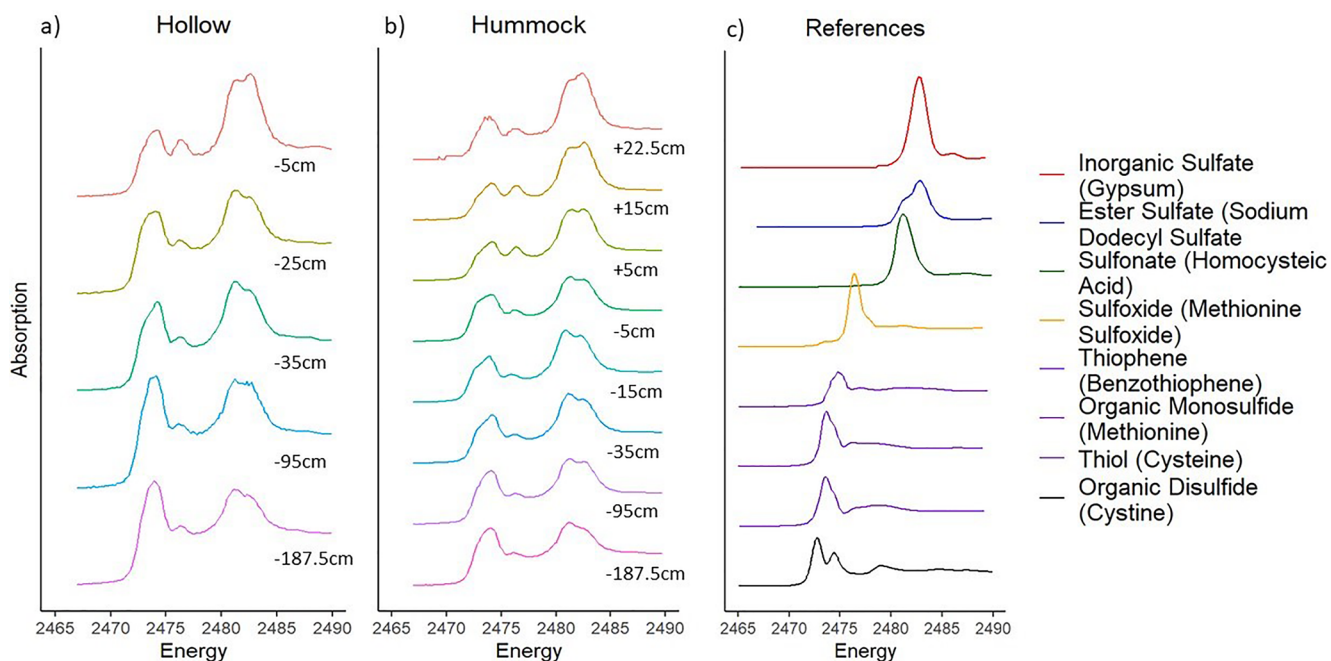


Figure 1. Sulfur 1s XANES spectra from hollow (a), hummock (b), and references that were detected in the samples (c). References are color-coded according to bin type—thiophenes, organic monosulfides, and thiols are binned together.

2600 according to US Environmental Protection Agency (EPA) method 1631.⁶¹

Methylmercury concentrations were measured by EPA Method 1630⁶² by distillation, ethylation, capillary gas chromatography, and CVAFS on a Tekran 2700. The detection limit was 0.03 ng g⁻¹ for THg analyses and 0.006 ng g⁻¹ for MeHg analyses.

2.6. Instantaneous Mercury Methylation and Demethylation Rate Constants. Rates were determined by incubating peat with simultaneous additions of enriched-abundance ²⁰⁰Hg²⁺ (94.3%) and Me²⁰¹Hg⁺ (84.7%) as outlined in Mitchell and Gilmour (2008).²⁹ See the [Supporting Information](#) for detailed methods.

Analytical quality control and assurance measures can be found in [Table S2](#): potential rate constant quality control and assurance measures. Potential rate constants for Hg²⁺ methylation (k_m) were calculated using the excess concentration of enriched ²⁰⁰Hg²⁺ that was methylated over the course of the incubation period with respect to the concentration of excess T²⁰⁰Hg in the sample.^{63,64} Potential MeHg demethylation rate constants (k_d) were determined assuming first-order reaction kinetics according to Lehnher et al. (2012).⁶⁵

2.7. *hgcAB* Primer Sequencing. Genomic DNA (gDNA) was isolated from the peat samples, quantified using Qubit (Thermo Fisher Scientific), and assessed for quality with NanoDrop One (Thermo Fisher Scientific). See the [Supporting Information](#) for detailed methods. The gene sequence *hgcAB* was amplified by the method described by Gionfriddo et al. (2020)⁶⁶ and clone libraries were created. The environmental clone *hgcA* sequences from this study were previously published as part of a study testing methods for identifying Hg-methylation genes from environmental samples and are publicly available under the NCBI GenBank accession numbers MT122211–MT122438.⁶⁶

There could be bias in these methods (amplifying, cloning, and sequencing *hgcA*) introduced by the choice of primer

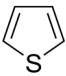
sequence. Primer sequences are based on reference *hgcA* from known methylators and therefore may prefer certain microbial guilds, such as deltas and methanogens over firmicutes and acetogens. The interpretation of the phylogenetic analysis of these data is limited as metabolic groupings of the results were based on taxonomic prefixes and suffixes as opposed to identifying functional genes for sulfate reduction, iron reduction, and methanogenesis. We inferred sulfate-reducing mercury methylators based on the phylogenetic placement of the cloned sequence compared to reference sequences of known/predicted mercury methylators. Because the mercury methylation genes have been classified as deltaproteobacteria, we inferred that the mercury methylators are capable of sulfate reduction. These data are not quantitative and do not tell us whether any of the *hgc* genes were active, if some groups have higher rates of activity than others (e.g., small number of sulfur reducers but high activity), or whether the organisms were alive when the DNA was extracted. Our data simply identified the presence or absence of *hgcAB* genes.

2.8. Statistical Analysis. All statistical analyses were performed in R 3.6.3⁶⁷ using package agricolae (v1.3.2; function: LSD.test).⁶⁸ Statistical differences of linear models were determined using multiple comparison least significant difference,⁶⁹ p-adjustment of “none”, and a significance level of $p < 0.05$. The Shapiro–Wilks test was used to determine the normality of THg, MeHg, and percent MeHg. No averaging was performed and the data set comprised composited cores by depth. The data were not normal, so we examined relationships between mercury and sulfur species in peat by using Spearman’s rank correlation for nonlinear and non-parametric data with a significance level of $p < 0.05$.

3. RESULTS AND DISCUSSION

3.1. Depth Profiles in Peatland Soil—Mercury, Sulfur, and *hgcAB* Genes. Spectra from 58 samples were fit to reference spectra using linear combination fitting ([Table S3](#): proportions of sulfur species for hummocks and [S4](#):

Table 1. Sulfur Species in the Reference Database

Reference compound	Functional group	Structure	Electronic oxidation state ^a	Group	Peak maxima (eV)	Source
L-Cystine	Organic disulfide	R-S-S-R'	-0.4		2472.8 / 2474.5	d.
L-Cysteine	Thiol	R-S-H	+0.2		2473.6	d.
Reduced S						
L-Methionine	Organic monosulfide	R-S-R'	+0.3		2473.6	d.
Benzothiophene and Bithiophene	Thiophene		+1.0		2473.7 / 2474.6	e., f.
Methionine Sulfoxide	Sulfoxide	R-S(O)-R'	+2		2476.3	d.
Sulfite	Sulfite	Na ₂ SO ₃	+4		2478.5	g., h.
Saccharin	Sulfone	R-SO ₂ -R'	+4		2480.0	f.
Oxidized S						
DL-Homocysteic acid ^b and ANSA ^c	Sulfonate	R-SO ₃ -H	+5		2481.2	d., h.
Gypsum	Inorganic sulfate	CaSO ₄	+6		2482.7	f.
Sodium dodecyl sulfate	Ester sulfate	R-O-SO ₃ -H	+6		2482.8	d.

^aOxidation state calculated and published in Cron et al. 2020. ^bDL-Homocysteic acid. ^c1-Amino-2-naphthol-4-sulfonic acid. ^dCron et al. 2020. ^eBehyan et al. 2013. ^fPierce et al. 2021. ^gManceau and Nagy 2012. ^hZeng et al. 2013.

proportions of sulfur species for hollows). Representative sulfur XANES spectra are shown in Figure 1.

Almost all sulfur detected in the S1 bog peat with sulfur XANES spectroscopy was in an organic form (Table S5: mean sulfur speciation by depth). Reduced organic sulfur species (having valence states of $\leq +1$, Table 1) comprised 42–72% of total sulfur over the full depth profile (+20 to –200 cm, Table S5: mean sulfur speciation by depth) which is consistent with past studies of boreal peatlands.⁷⁰ The oxidized sulfur species (valence states $\geq +2$) decreased with depth ($p < 0.05$), while reduced sulfur species (valence states $\leq +1$) increased with depth ($p < 0.05$). The lowest percentages of reduced sulfur species were observed in surface samples from both hollows (–5 cm, 48% on average) and hummocks (+15 cm, 42% on average; Figure 2 and Table S5: mean sulfur speciation by depth).

Various organic sulfur species with different electronic states (–0.4 to +6) were measured in living *Sphagnum* (Table S5: mean sulfur speciation by depth). Sulfur speciation in *Sphagnum* tissues was similar between *S. divinum* and *S. angustifolium/fallax*. The main difference between the two was that *S. divinum* accumulated more inorganic sulfate, whereas *S. angustifolium/fallax* accumulated more ester sulfate. However, only one sample per *Sphagnum* type was measured, so the potential variability in sulfur speciation was not addressed.

Within the acrotelm and mesotelm, concentrations of sulfur species were variable and in the catotelm, the concentrations

were constant. In this study, our observations are consistent with the published literature^{30,34} that shows that the depth interval from –5 to –35 cm is a biogeochemically active zone, which overlaps the range of water table depth fluctuations (Figure 2). Maxima in total sulfur, organic disulfide, THg, MeHg, percent MeHg, and major changes in the composition of the sulfur organic compounds all occurred in this zone (Figures 2, 3, and S2: depth profiles of mean THg and percent MeHg). Subsurface maximum in organic sulfur concentration in peatlands may result from sulfate reduction processes occurring where perennial saturation most often occurs.⁷¹ Our findings are consistent with previous reports of subsurface maxima in total sulfur and MeHg that correspond to the mesotelm.^{30,34,46,71,72} It has been proposed that this maximum in MeHg in the zone of water table fluctuation is due to sulfur cycling between reduced and oxidized forms as the redox conditions change with the water table.^{15,31,33,73,74} This internal cycling of sulfur can drive MeHg production with minimal atmospheric deposition of new sulfate.

Both THg and MeHg concentrations were relatively low in surficial peat and peaked at depths between –25 and –35 cm in the hollows and at –5 cm in the hummocks (Figures 2 and S2: depth profiles of mean THg and percent MeHg, Table S6: mean mercury concentrations by depth). The shape of the MeHg profile is directly influenced by microbial activity. In contrast, the shape of the THg profile is determined primarily by atmospheric deposition and indirectly influenced by

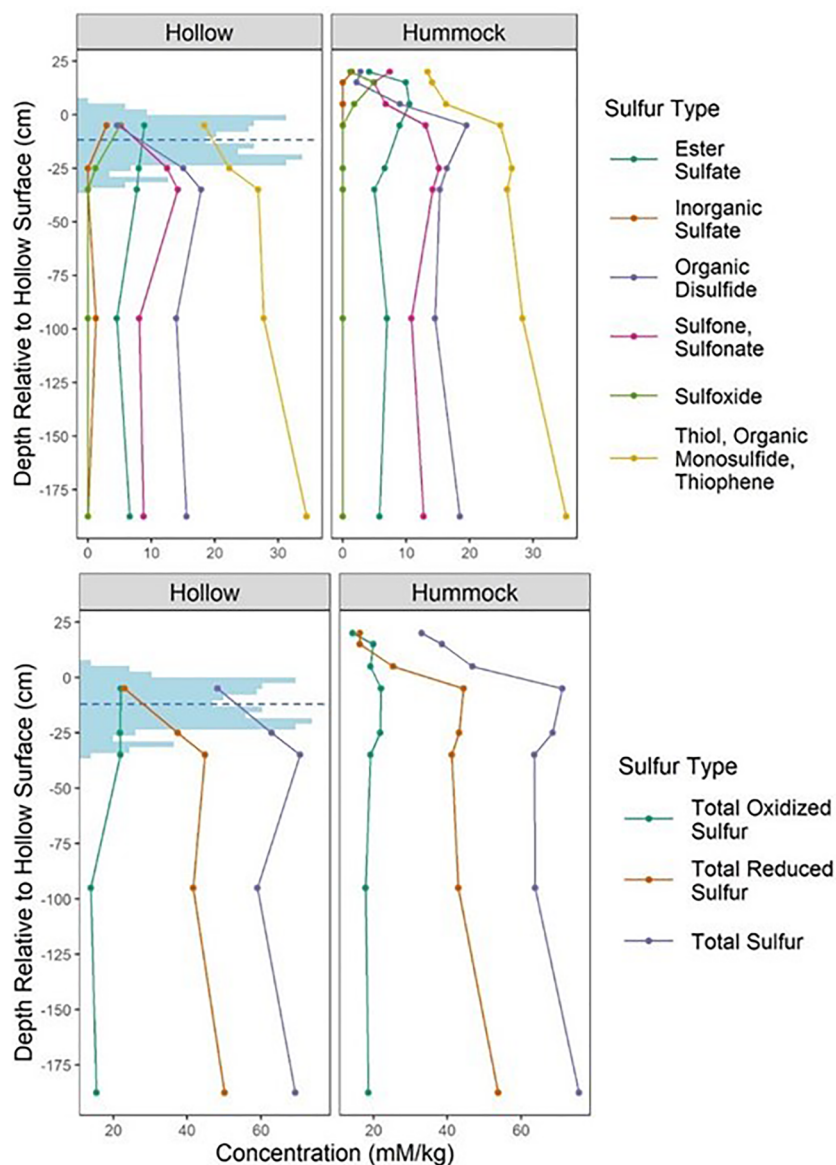


Figure 2. Depth profiles of sulfur concentration and speciation. Top Panel: inorganic sulfate (orange), ester sulfate (teal), sulfone and sulfonate (pink), sulfoxide (green), thiol and thiophene and organic monosulfide (yellow), and organic disulfide (purple), as measured by XANES spectroscopy. Bottom Panel: total oxidized sulfur (teal) is the sum of inorganic sulfate, ester sulfate, sulfone, sulfonate, and sulfoxide. Total reduced sulfur (orange) is the sum of thiol, organic monosulfide, thiophene, and organic disulfide. Blue-shaded area is a histogram showing the range of daily water table positions (minimum: -35 cm, maximum: $+6$ cm) in 2012. Blue dashed line is the water table height on the day of sampling.

microbial activity. Mercury emissions greatly increased during the industrial revolution (~ 1850) through the 1970s,⁷⁵ which corresponds to increased atmospheric deposition in depths -25 to -100 cm (hollows, Figure S2: depth profiles of mean THg and percent MeHg). Microbial decomposition of the peat increases the concentration of THg by decreasing the mass of carbon and the volume of peat.⁷⁶ In the surface depths, 1 cm of peat may correlate to 1 year of deposition, whereas in the deeper peat, 1 cm may correlate to several hundred years.⁷⁶ Total mercury and MeHg concentrations decreased below -35 cm depth (Figures 3 and S2: depth profiles of mean THg and percent MeHg, Table S6: mean mercury concentrations by depth). Our hummock, near-surface, THg concentrations were approximately 50 ng g^{-1} which is consistent with a hummock depth profile measured at a similar bog in northern Minnesota by Benoit et al. (1998) as well as having similar depths for concentration maxima.⁷⁵ These same similarities, but for

hollows, were found with the THg depth profiles in Givélet et al. (2003) located in southern Ontario, Canada.⁷⁷ Average percent MeHg levels (i.e., MeHg concentrations expressed as a percentage of THg concentrations) were less than 2.6% throughout peat cores and peaked at depths -35 and -5 cm for hollows and hummocks, respectively.

No relationship was found between the presence of *hgcAB* genes and the MeHg profile because the *hgcAB* genes are detected at all depths even where MeHg concentrations are low. The data do not provide quantitative information, so the overall abundance of *hgcAB* in the mesotelm is unknown. Many factors may impact MeHg distribution besides the presence of mercury methylators, including their activity and abundance, which were not measured. A recent study showed no significant correlation between the gene abundance of *hgcAB* (qPCR or metagenomic-based methods) and THg or MeHg concentrations across diverse environments such as

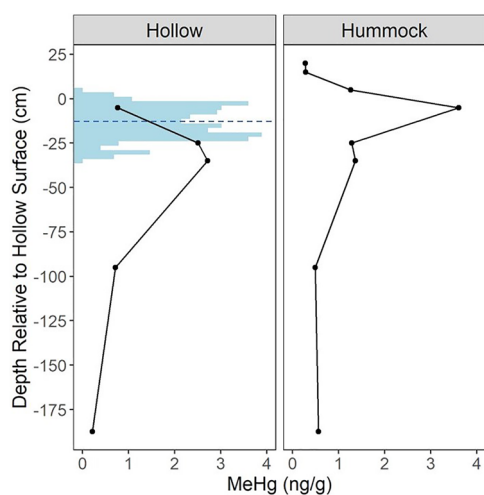


Figure 3. Depth profile of mean MeHg concentrations in peat for cores collected from hummocks and hollows. Blue-shaded area is a histogram of the range of water table positions in 2012. Blue dashed line is the water table height on the day of sampling. Total mercury and percent MeHg depth profiles are provided in the [Supporting Information](#) (Figure S2).

riverine areas, tidal marshes, and arctic permafrost.⁷⁸ Generally, the potential for microbial methylation of mercury appears to be present throughout the peat profile. There are several caveats to these data. First, the methods do not give a quantitative assessment of *hgcAB* genes across depth. Second, no overall measure of biomass was collected to assess microbial abundance. Third, sequencing was not deep enough (i.e., only five or so clones per depth) to capture the full diversity in *hgcA* genes that were present in the clone libraries. However, the collation of clones from each depth and sample site gives us a glimpse of mercury methylator diversity at this site. An area for future investigation is to perform metagenomic sequencing techniques or higher throughput sequencing of *hgcAB* amplicons to overcome these caveats.

3.2. Organic Disulfide is a Product of Mercury Methylation. The depth profiles of mercury concentrations and sulfur species were consistent among cores for soils having similar microtopography (e.g., all hummock profiles are similar). The most distinguishing feature of all sulfur speciation profiles was a maximum concentration of organic disulfide in near-surface peat (within ~30 cm of the surface for both hummocks and hollows; [Figure 2](#)). Within the zone of water table fluctuation, concentration maxima of MeHg and organic disulfide co-occur for both hollows and hummocks. Methylmercury and percent MeHg were both positively correlated with organic disulfide throughout the depth profile in hummocks but not hollows ($R_{\text{Spearman}} = 0.62$, [Table S7](#): Spearman's correlations between sulfur species and mercury). We performed a statistical correlation analysis and interpret these results based on well-established chemical and biological processes.

Hummocks are elevated approximately 30 cm above the hollows ([Figure 2](#)) but the absolute water table occurs at the same absolute elevation in both, with the result that the surface layers of hummocks are more oxic than in hollows.^{43,79} The maximum in MeHg, total sulfur, and organic disulfide concentrations in hummocks and hollows occur at the same depths from the microtopographic surface (−35 cm, [Figures 2 and 3](#)). This indicates that the biogeochemical environment

(e.g., soil moisture, redox potential, and biophysical properties) in the mesotelm varies with surface microtopography.⁸⁰ There may well be a biogeochemical reason for the significant correlation between MeHg and organic disulfide in hummocks, but not hollows. It is also possible that our sampling scheme did not allow us to resolve that relationship in hollows because the sampling interval increased from 10 to 60 cm at −35 cm below the hollow surface.

Microbial sulfate reduction produces chemically reduced forms of sulfur, such as hydrogen sulfide.^{17,81} Hydrogen sulfide and other forms of sulfur are known to be reactive with organic matter in a variety of natural settings through processes referred to as sulfurization or sulfidization reactions.^{26,82–84} Organic disulfide is a possible end-product of microbial sulfate reduction processes in peatlands and may be a co-product with MeHg.^{30,71,85} There is evidence that SRB are present at our study site at depths −30 to −50 cm.^{86,87} The 2014 studies by Lin et al.^{86,87} were performed at our research site and were generic to all microorganisms in the peat, meaning it differs from ours in that we selected a subset of microorganisms that had the *hgcAB* gene. Microbes containing the *hgcAB* gene comprise less than 5% of the general microbial community across various environment types.⁷⁸ Based on interpreting the *hgcA* phylogenetic classification as sulfate reducers, we saw SRB that contain the genes for mercury methylation, *hgcAB*, at depths +5 cm through −10 cm for the hummock locations only ([Figure S3](#): depth profile of the presence of *hgcAB* and binned microbiological taxa). Not surprisingly, the majority of the genes detected were binned in the “uncultured” and “other” group and so little information can be gleaned as to what geochemical or physico-chemical conditions would allow the organisms possessing these genes to thrive and be biochemically active.

3.3. Thiols, Monosulfides, Thiophenes, and Mercury Bioavailability. Unlike organic disulfides, the organic monosulfides (thiols, monosulfides, and thiophenes) were negatively correlated with MeHg ($R_{\text{Spearman}} = -0.60$ and -0.51 , hollows and hummocks, respectively) and displayed a maximum in the catotelm where THg and MeHg are low ([Figures 2, 3, and S2](#): depth profiles of mean THg and percent MeHg, and [Table S7](#): Spearman's correlations between sulfur species and mercury). Thiol functional groups in dissolved and particulate organic pools are known to bind to mercury strongly.^{20,29,88,89} Studies using extended X-ray absorption fine structure (EXAFS) spectroscopy show that thiol moieties in organic matter form ligand complexes with Hg(II) and CH_3Hg^+ which increases THg and MeHg storage in peatland soil.^{20,90–92} In the aqueous phase, thiols introduced as soluble cysteine desorb Hg(II) from the solid phase into the porewaters.⁹³ While the chemical affinity between mercury and thiols is well demonstrated, the effect of thiols on MeHg production by microorganisms appears to be species and compound specific. Mercury methylating microorganisms such as *Pseudodesulfovibrio mercurii* ND132 (previously *D. desulfuricans* ND132) exhibit enhanced methylation in the presence of all thiols, whereas *G. sulfurreducens* PCA's methylating ability is enhanced by small molecular thiols (e.g., cysteine and mercaptopropionate) and inhibited by larger molecular thiols (e.g., glutathione and penicillamine).^{93–96} The observed negative correlation between thiols and MeHg in peat is consistent with a reduction in the methylation activity in the porewaters in the presence of solid-state thiols. This finding is further supported by the observed negative correlation in the

peat between thiols and the ratio of methylation rate constants (k_m) to demethylation rate constants (k_d) ($R_{\text{Spearman}} = -0.37$, Table S8: Spearman's correlations between sulfur species and potential methylation rate constants). To our knowledge, this is the first finding of this kind outside of a laboratory setting. It is possible that the strong binding affinity between thiols in peat and Hg(II) causes a reduction in the bioavailability for methylation in the porewaters. As opposed to peatland soil, studies of porewater have found a positive relationship between k_m and small molecular thiols.⁹⁷ It should be noted that in the deep peat, organic monosulfides are not causing a decrease in MeHg. Methylmercury is low in the catotelm because THg concentrations are low. The deep peat is also characterized by lower microbial activity at depths due to environmental conditions. Organic monosulfides in the peatland soil affecting the bioavailability of mercury in the porewater are likely restricted to the acrotelm and mesotelm.

3.4. Ester Sulfate as a Potential Substrate for Sulfur-Reducing Mercury Methylators. The depths at which the greatest average methylation rate constant, k_m , occurred was -10 to -20 cm and corresponded with the depth of the MeHg concentration maximum (Figures 3 and 4a). Within the mesotelm, there was high variability in k_m . The demethylation rate constant is variable among replicates and has no significant differences with depth, so the depth profile can be considered flat (Figure 4b). The greatest net methylation potential, based on the ratio of k_m to k_d , would occur at -10 to -20 cm depth, whereas the greatest net demethylation potential would occur above and below those depths (Figure 4c). Between 2002 and 2012, the water table at the S1 bog is most often located between 0 and -30 cm.⁹⁸

Total mercury concentration and methylation rate constant values are strongly and positively correlated ($R_{\text{Spearman}} = 0.86$, p -value < 0.05 (Figure S4: THg comparison plots with rate data) and this correlation is consistent with previous findings.^{99,100} Total mercury concentration and demethylation rate constant values are moderately and negatively correlated ($R_{\text{Spearman}} = -0.41$, p -value < 0.05 , Figure S4: THg comparison plots with rate data). Methylmercury concentration and the methylation rate constant values are strongly and positively correlated ($R_{\text{Spearman}} = 0.67$, p -value < 0.05 , Figure S5: MeHg comparison plots with rate data). This positive correlation is consistent with a past study based in saltwater marshes where the correlation between percent MeHg of THg and the methylation rate constant was $R_{\text{Spearman}} = 0.80$.²⁹ Methylmercury concentration and the demethylation rate constant values are weakly and negatively correlated ($R_{\text{Spearman}} = -0.39$, p -value < 0.05 , Figure S5: MeHg comparison plots with rate data).

A unique finding in this study is that k_m was positively correlated to total oxidized organic sulfur species and ester sulfate in peat ($R_{\text{Spearman}} = 0.38$ and 0.56 , respectively). The positive correlation between ester sulfate and k_m provides evidence for ester sulfate being the reactant in the microbially mediated methylation process via sulfate reduction. Inorganic sulfate was detected in a few of the samples but was not common (Tables S3: proportions of sulfur species for hummocks and S4: proportions of sulfur species for hollows). This finding is consistent with past studies that showed that ester sulfate can be utilized by SRB as a terminal electron acceptor in the absence of inorganic sulfate.^{17,101–103} Porewater sulfate pools are low ($\text{sub-}\mu\text{mol L}^{-1}$, Figure S6: depth profiles of mean porewater chemistry), so the positive correlation between k_m and solid-phase ester sulfate may

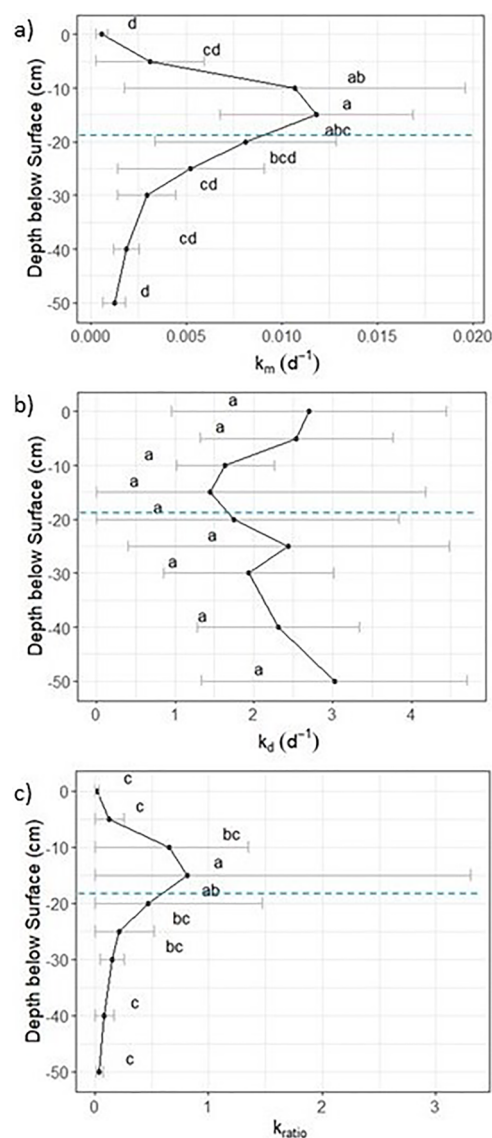


Figure 4. Rate constant profiles from the S1 bog, August 2016. Rate constant (k_m) is the potential methylation constant (a), k_d is the potential demethylation constant (b), and k_{ratio} is calculated as $k_m \div k_d \times 100$ (c). Error bars are 95% confidence intervals. Means with the same letter are not statistically different from each other ($p \geq 0.05$). Blue dashed line is the water table height on the day of sampling.

indicate that the solid-phase sulfur pools, which have a much larger sulfur concentration range, may be available to microbial activity or exchanging with the porewaters. Congruently, k_m was negatively correlated with total reduced sulfur species ($R_{\text{Spearman}} = -0.38$), indicating that as sulfur is reduced, along with producing MeHg, potential methylation rates decrease.

A variety of biogeochemical pools and processes contribute to the abundance and speciation of sulfur and mercury in an ombrotrophic peatland. Microorganisms and plants immobilize atmospherically deposited sulfate as organic sulfur species through assimilatory and dissimilatory sulfate reduction.^{104–107} Sulfate-reducing microbes are known to link sulfate reduction to the formation of reactive hydrogen sulfide ($\text{H}_2\text{S}_{\text{aq}}$) and mercury methylation.^{24,82,108,109} Several lines of evidence in our findings suggest that dissimilatory sulfate reduction processes were important in the subsurface peat. Porewater sulfate concentrations in hollows revealed a substantial

decrease from 0 to -50 cm and high variability at -30 cm (Figure S6: depth profiles of mean porewater chemistry). At the same time, porewater profiles of total dissolved sulfide ($\text{H}_2\text{S}_{\text{aq}}$ and HS^-_{aq}) showed maxima at -30 cm, suggesting the occurrence of sulfate reduction processes at this depth (Figure S6: depth profiles of mean porewater chemistry). As MeHg is produced as a co-product with hydrogen sulfide, similar depths of maximum MeHg concentrations and maximum reduced sulfur species are expected and substantiated by our data (Figures 2 and 3). Drying of peatland soils during low water table events may oxidize these organic sulfur compounds and provide sulfate to fuel net MeHg production following subsequent wetting events.¹⁵ Thus, dry-to-wet cycles can liberate sulfate and create the potential for increased MeHg fluxes to surface waters.^{15,31,110,111}

Our findings will serve as a time zero characterization of the SPRUCE project, a large-scale temperature and elevated CO_2 manipulation experiment, which was fully initiated in 2016. We anticipate that projected climate changes in the northern hemispheric boreal ecotone will change mercury release from peatlands to downstream aquatic ecosystems and the atmosphere. For instance, climate change and its associated effects on water table fluctuations may drive the subsurface maxima in reduced organic sulfur concentrations, MeHg concentrations, and microbial activity deeper into the peat. The net effect of these changes on mercury fluxes from peatlands under climate warming is currently under investigation.

■ ASSOCIATED CONTENT

SI Supporting Information

The Supporting Information is available free of charge at <https://pubs.acs.org/doi/10.1021/acs.est.1c04662>.

Impact of water table height; detailed methods; map showing the MEF within Minnesota and the research site within MEF; depth profiles; *hgcAB* gene presence by the binned group; THg comparison plots and MeHg comparison plots of rate data; complete list of sulfur reference compounds; potential rate constant quality control and assurance measures; proportions of sulfur species as calculated by linear combination fitting; mean sulfur speciation; mean mercury concentrations; Spearman's correlations between sulfur species and mercury and between sulfur species and potential methylation rate constants; and mean potential rate constants (PDF)

■ AUTHOR INFORMATION

Corresponding Author

Brandy M. Toner – Department of Soil, Water, and Climate, University of Minnesota, St. Paul, Minnesota 55108, United States; orcid.org/0000-0002-3681-3455; Email: toner@umn.edu

Authors

Caroline E. Pierce – Department of Soil, Water, and Climate, University of Minnesota, St. Paul, Minnesota 55108, United States

Olha S. Furman – Department of Soil, Water, and Climate, University of Minnesota, St. Paul, Minnesota 55108, United States; Present Address: Department of Agriculture, Water, and the Environment, Australian Government, Canberra, Australia

Sarah L. Nicholas – Department of Soil, Water, and Climate, University of Minnesota, St. Paul, Minnesota 55108, United States; Present Address: Brookhaven National Laboratory–National Synchrotron Light Source II, Upton, NY 11973 USA.

Jill Coleman Wasik – Plant and Earth Science Department, University of Wisconsin River Falls, River Falls, Wisconsin 54022, United States

Caitlin M. Gionfriddo – Biosciences Division, Oak Ridge National Laboratory, Oak Ridge, Tennessee 37831, United States; Present Address: Smithsonian Environmental Research Center, Edgewater, MD 21037 USA.

Ann M. Wymore – Biosciences Division, Oak Ridge National Laboratory, Oak Ridge, Tennessee 37831, United States

Stephen D. Sebestyen – USDA Forest Service, Northern Research Station, Grand Rapids, Minnesota 55744, United States; orcid.org/0000-0002-6315-0108

Randall K. Kolka – USDA Forest Service, Northern Research Station, Grand Rapids, Minnesota 55744, United States

Carl P. J. Mitchell – Department of Physical and Environmental Sciences, University of Toronto Scarborough, Toronto, Ontario M1C 1A4, Canada; orcid.org/0000-0001-8538-5138

Natalie A. Griffiths – Environmental Sciences Division, Oak Ridge National Laboratory, Oak Ridge, Tennessee 37831, United States; orcid.org/0000-0003-0068-7714

Dwayne A. Elias – Biosciences Division, Oak Ridge National Laboratory, Oak Ridge, Tennessee 37831, United States; orcid.org/0000-0002-4469-6391

Edward A. Nater – Department of Soil, Water, and Climate, University of Minnesota, St. Paul, Minnesota 55108, United States

Complete contact information is available at: <https://pubs.acs.org/doi/10.1021/acs.est.1c04662>

Notes

The authors declare no competing financial interest.

■ ACKNOWLEDGMENTS

Funding from the National Science Foundation Graduate Research Fellowship supported Caroline Pierce. Funding from the US Department of Energy (DOE) and USDA Forest Service Northern Research Station supported O.S.F. A portion of the work performed at Oak Ridge National Laboratory was sponsored by the DOE Office of Biological and Environmental Research, Office of Science (OBER), as part of the Mercury Science Focus Area which is managed by UT-Battelle LLC for the DOE under contract DE-AC05-00OR22725. We thank Nate Aspelin for assistance with porewater sampling; Michael Ottman, Michelle Natarajan, Trudy Bolin, and Tianpin Wu for beamtime assistance at the APS 9-BM; Yongfeng Hu, Qunfeng Xiao, and Aimee MacLennan for beamtime assistance at the CLS SXRMB; Sona Psarska, Reba Van Beusekom, and Mikhail Mack for assistance with MeHg measurements; and Kevin Ng, Steven Chang, and Haiyong Huang for assistance with the methylation and demethylation rate assays. Funding for the methylation and demethylation rate assays were provided by the Natural Sciences and Engineering Research Council of Canada. Acid volatile sulfur concentrations were measured at the St. Croix Watershed Research Station, Science Museum of Minnesota. A portion of the work was conducted at (1) the APS, a DOE user facility operated for the DOE Office of

Science by Argonne National Laboratory under Contract no. DE-AC02-06CH11357, and (2) the CLS, which is supported by the Canadian Foundation for Innovation, Natural Sciences and Engineering Research Council of Canada, the University of Saskatchewan, the Government of Saskatchewan, Western Economic Diversification Canada, the National Research Council Canada, and the Canadian Institutes of Health Research. The SPRUCE experiment is supported by the DOE OBER and is a collaborative research between Oak Ridge National Laboratory and the USDA Forest Service. USDA Forest Service funds support the long-term research program at the Marcell Experimental Forest and the participation of R.K.K. and S.D.S. in this research. N.A.G. was supported by DOE OBER.

REFERENCES

- (1) Yu, Z.; Loisel, J.; Brosseau, D. P.; Beilman, D. W.; Hunt, S. J. Global Peatland Dynamics since the Last Glacial Maximum. *Geophys. Res. Lett.* **2010**, *37*, L13402.
- (2) Krause, L.; McCullough, K. J.; Kane, E. S.; Kolka, R. K.; Chimner, R. A.; Lilleskov, E. A. Impacts of Historical Ditching on Peat Volume and Carbon in Northern Minnesota USA Peatlands. *J. Environ. Manage.* **2021**, *296*, 113090.
- (3) Grigal, D. F. Mercury Sequestration in Forests and Peatlands: A Review. *J. Environ. Qual.* **2003**, *32*, 393–405.
- (4) Mitchell, C. P. J.; Branfireun, B. A.; Kolka, R. K. Spatial Characteristics of Net Methylmercury Production Hot Spots in Peatlands. *Environ. Sci. Technol.* **2008**, *42*, 1010–1016.
- (5) Kolka, R. K.; Sebestyen, S. D.; Verry, E. S.; Brooks, K. N. Mercury Cycling in Peatland Watersheds in Peatland Biogeochemistry and Watershed Hydrology. *Peatland Biogeochemistry and Watershed Hydrology at the Marcell Experimental Forest*; CRC Press, 2011; pp 349–370.
- (6) Ullrich, S. M.; Tanton, T. W.; Abdrashitova, S. A. Mercury in the Aquatic Environment: A Review of Factors Affecting Methylation. *Crit. Rev. Environ. Sci. Technol.* **2001**, *31*, 241–293.
- (7) Gilmour, C. C.; Podar, M.; Bullock, A. L.; Graham, A. M.; Brown, S. D.; Somenahally, A. C.; Johs, A.; Hurt, R. A.; Bailey, K. L.; Elias, D. A. Mercury Methylation by Novel Microorganisms from New Environments. *Environ. Sci. Technol.* **2013**, *47*, 11810–11820.
- (8) Jeremiason, J. D.; Engstrom, D. R.; Swain, E. B.; Nater, E. A.; Johnson, B. M.; Almendinger, J. E.; Monson, B. A.; Kolka, R. K. Sulfate Addition Increases Methylmercury Production in an Experimental Wetland. *Environ. Sci. Technol.* **2006**, *40*, 3800–3806.
- (9) Coleman Wasik, J. K.; Mitchell, C. P. J.; Engstrom, D. R.; Swain, E. B.; Monson, B. A.; Balogh, S. J.; Jeremiason, J. D.; Branfireun, B. A.; Eggert, S. L.; Kolka, R. K.; Almendinger, J. E. Methylmercury Declines in a Boreal Peatland When Experimental Sulfate Deposition Decreases. *Environ. Sci. Technol.* **2012**, *46*, 6663–6671.
- (10) Poulain, A. J.; Barkay, T. Cracking the Mercury Methylation Code. *Science* **2013**, *339*, 1280–1281.
- (11) Kronberg, R.-M.; Schaefer, J. K.; Björn, E.; Skjellberg, U. Mechanisms of Methyl Mercury Net Degradation in Alder Swamps: The Role of Methanogens and Abiotic Processes. *Environ. Sci. Technol. Lett.* **2018**, *5*, 220–225.
- (12) Bae, H. S.; Dierberg, F. E.; Ogram, A. Periphyton and Flocculent Materials Are Important Ecological Compartments Supporting Abundant and Diverse Mercury Methylator Assemblages in the Florida Everglades. *Appl. Environ. Microbiol.* **2019**, *85*, No. e00156-19.
- (13) Regnell, O.; Watras, C. J. Microbial Mercury Methylation in Aquatic Environments: A Critical Review of Published Field and Laboratory Studies. *Environ. Sci. Technol.* **2019**, *53*, 4–19.
- (14) Qian, C.; Chen, H.; Johs, A.; Lu, X.; An, J.; Pierce, E. M.; Parks, J. M.; Elias, D. A.; Hettich, R. L.; Gu, B. Quantitative Proteomic Analysis of Biological Processes and Responses of the Bacterium *Desulfovibrio Desulfuricans* ND132 upon Deletion of Its Mercury Methylation Genes. *Proteomics* **2018**, *18*, 1700479.
- (15) Coleman Wasik, J. K.; Engstrom, D. R.; Mitchell, C. P. J.; Swain, E. B.; Monson, B. A.; Balogh, S. J.; Jeremiason, J. D.; Branfireun, B. A.; Kolka, R. K.; Almendinger, J. E. The Effects of Hydrologic Fluctuation and Sulfate Regeneration on Mercury Cycling in an Experimental Peatland. *J. Geophys. Res.: Biogeosci.* **2015**, *120*, 1697–1715.
- (16) Kolka, R. K.; Grigal, D. F.; Nater, E. A.; Verry, E. S. Hydrologic Cycling of Mercury and Organic Carbon in a Forested Upland–Bog Watershed. *Soil Sci. Soc. Am. J.* **2001**, *65*, 897–905.
- (17) Pester, M.; Knorr, K.; Friedrich, M. W.; Wagner, M.; Loy, A. Sulfate-Reducing Microorganisms in Wetlands – Fameless Actors in Carbon Cycling and Climate Change. *Front. Microbiol.* **2012**, *3*, 72.
- (18) Åkerblom, S.; Bishop, K.; Björn, E.; Lambertsson, L.; Eriksson, T.; Nilsson, M. B. Significant Interaction Effects from Sulfate Deposition and Climate on Sulfur Concentrations Constitute Major Controls on Methylmercury Production in Peatlands. *Geochim. Cosmochim. Acta* **2013**, *102*, 1–11.
- (19) Nagy, K. L.; Manceau, A.; Gasper, J. D.; Ryan, J. N.; Aiken, G. R. Metallothionein-Like Multinuclear Clusters of Mercury (II) and Sulfur in Peat. *Environ. Sci. Technol.* **2011**, *45*, 7298–7306.
- (20) Manceau, A.; Nagy, K. L. Relationships between Hg(II)-S Bond Distance and Hg(II) Coordination in Thiolates. *Dalton Trans.* **2008**, *11*, 1421–1425.
- (21) Skjellberg, U. Competition among Thiols and Inorganic Sulfides and Polysulfides for Hg and MeHg in Wetland Soils and Sediments under Suboxic Conditions: Illumination of Controversies and Implications for MeHg Net Production. *J. Geophys. Res.* **2008**, *113*, G00C03.
- (22) Mitchell, C. P. J.; Branfireun, B. A.; Kolka, R. K. Assessing Sulfate and Carbon Controls on Net Methylmercury Production in Peatlands: An in Situ Mesocosm Approach. *Appl. Geochem.* **2008**, *23*, 503–518.
- (23) Åkerblom, S.; Nilsson, M. B.; Skjellberg, U.; Björn, E.; Jonsson, S.; Ranneby, B.; Bishop, K. Formation and Mobilization of Methylmercury across Natural and Experimental Sulfur Deposition Gradients. *Environ. Pollut.* **2020**, *263*, 114398.
- (24) Blodau, C.; Mayer, B.; Peiffer, S.; Moore, T. R. Support for an Anaerobic Sulfur Cycle in Two Canadian Peatland Soils. *J. Geophys. Res.* **2007**, *112*, G02004.
- (25) Urban, N. R.; Eisenreich, S. J.; Grigal, D. F. Sulfur Cycling in a Forested Sphagnum Bog in Northern Minnesota. *Biogeochemistry* **1989**, *7*, 81–109.
- (26) Fakhraee, M.; Li, J.; Katsev, S. Significant Role of Organic Sulfur in Supporting Sedimentary Sulfate Reduction in Low-Sulfate Environments. *Geochim. Cosmochim. Acta* **2017**, *213*, 502–516.
- (27) Jochum, L. M.; Schreiber, L.; Marshall, I. P. G.; Jørgensen, B. B.; Schramm, A.; Kjeldsen, K. U. Single-Cell Genomics Reveals a Diverse Metabolic Potential of Uncultivated *Desulfatiglans*-Related Deltaproteobacteria Widely Distributed in Marine Sediment. *Front. Microbiol.* **2018**, *9*, 2038.
- (28) Parks, J. M.; Johs, A.; Podar, M.; Bridou, R.; Hurt, R. A.; Smith, S. D.; Tomanicek, S. J.; Qian, Y.; Brown, S. D.; Brandt, C. C.; Palumbo, A. V.; Smith, J. C.; Wall, J. D.; Elias, D. A.; Liang, L. The Genetic Basis for Bacterial Mercury Methylation. *Science* **2013**, *339*, 1332–1335.
- (29) Mitchell, C. P. J.; Gilmour, C. C. Methylmercury Production in a Chesapeake Bay Salt Marsh. *J. Geophys. Res.* **2008**, *113*, G00C04–14.
- (30) Novák, M.; Wieder, R. K. Inorganic and Organic Sulfur Profiles in Nine Sphagnum Peat Bogs in the United States and Czechoslovakia. *Water, Air, Soil Pollut.* **1992**, *65*, 353–369.
- (31) Rolffhus, K. R.; Hurley, J. P.; Bodaly, R. A.; Perrine, G. Production and Retention of Methylmercury in Inundated Boreal Forest Soils. *Environ. Sci. Technol.* **2015**, *49*, 3482–3489.
- (32) Haynes, K. M.; Kane, E. S.; Potvin, L.; Lilleskov, E. A.; Kolka, R. K.; Mitchell, C. P. J. Gaseous Mercury Fluxes in Peatlands and the

- Potential Influence of Climate Change. *Atmos. Environ.* **2017**, *154*, 247–259.
- (33) Haynes, K. M.; Kane, E. S.; Potvin, L.; Lilleskov, E. A.; Kolka, R. K.; Mitchell, C. P. J. Mobility and Transport of Mercury and Methylmercury in Peat as a Function of Changes in Water Table Regime and Plant Functional Groups. *Global Biogeochem. Cycles* **2017**, *31*, 233–244.
- (34) Haynes, K. M.; Kane, E. S.; Potvin, L.; Lilleskov, E. A.; Kolka, R. K.; Mitchell, C. P. J. Impacts of Experimental Alteration of Water Table Regime and Vascular Plant Community Composition on Peat Mercury Profiles and Methylmercury Production. *Sci. Total Environ.* **2019**, *682*, 611–622.
- (35) Sirota, J. I.; Kolka, R. K.; Sebestyen, S. D.; Nater, E. A. Mercury Dynamics in the Pore Water of Peat Columns during Experimental Freezing and Thawing. *J. Environ. Qual.* **2020**, *49*, 404–416.
- (36) Shi, X.; Thornton, P. E.; Ricciuto, D. M.; Hanson, P. J.; Mao, J.; Sebestyen, S. D.; Griffiths, N. A.; Bisht, G. Representing Northern Peatland Microtopography and Hydrology within the Community Land Model. *Biogeosciences* **2015**, *12*, 6463–6477.
- (37) Gorham, E. Biotic Impoverishment in Northern Peatlands. In *Earth in Transition: Patterns and Process of Biotic Impoverishment*; Woodwell, G. M., Ed.; Cambridge University Press: New York, 1990; pp 65–98.
- (38) Glaser, P. H. *The Ecology of Patterned Boreal Peatlands of Northern Minnesota*; The Service, 1987.
- (39) Sebestyen, S. D.; Lany, N. K.; Roman, D. T.; Burdick, J. M.; Kyllander, R. L.; Verry, E. S.; Kolka, R. K. Hydrological and Meteorological Data from Research Catchments at the Marcell Experimental Forest. *Hydrol. Process.* **2021**, *35*, No. e14092.
- (40) Sebestyen, S.; Dorrance, C.; Olson, D.; Verry, E.; Kolka, R.; Elling, A.; Kyllander, R. Long-Term Monitoring Sites and Trends at the Marcell Experimental Forest. *Peatland Biogeochemistry and Watershed Hydrology at the Marcell Experimental Forest*; CRC Press, 2011; pp 15–71.
- (41) Parsekian, A. D.; Slater, L.; Ntarlagiannis, D.; Nolan, J.; Sebestyen, S. D.; Kolka, R. K.; Hanson, P. J. Uncertainty in Peat Volume and Soil Carbon Estimated Using Ground-Penetrating Radar and Probing. *Soil Sci. Soc. Am. J.* **2012**, *76*, 1911–1918.
- (42) Verry, E. S.; Brooks, K. N.; Nichols, D. S.; Ferris, D. R.; Sebestyen, S. D. Watershed Hydrology. *Peatland Biogeochemistry and Watershed Hydrology at the Marcell Experimental Forest*; CRC Press, 2011; pp 193–212.
- (43) Nungesser, M. K. Modelling Microtopography in Boreal Peatlands: Hummocks and Hollows. *Ecol. Model.* **2003**, *165*, 175–207.
- (44) Verry, E.; Boelter, D.; Päivänen, J.; Nichols, D.; Malterer, T.; Gafni, A. Physical Properties of Organic Soils. *Peatland Biogeochemistry and Watershed Hydrology at the Marcell Experimental Forest*; CRC Press, 2011; pp 135–176.
- (45) Tfaily, M. M.; Cooper, W. T.; Kostka, J. E.; Chanton, P. R.; Schadt, C. W.; Hanson, P. J.; Iversen, C. M.; Chanton, J. P. Organic Matter Transformation in the Peat Column at Marcell Experimental Forest: Humification and Vertical Stratification. *J. Geophys. Res.: Biogeosci.* **2014**, *119*, 661–675.
- (46) Clymo, R. S.; Bryant, C. L. Diffusion and Mass Flow of Dissolved Carbon Dioxide, Methane, and Dissolved Organic Carbon in a 7-m Deep Raised Peat Bog. *Geochim. Cosmochim. Acta* **2008**, *72*, 2048–2066.
- (47) Iversen, C. M.; Hansen, P.; Brice, D. J.; Phillips, J. R.; McFarlane, K. J.; Hobbie, E. A.; Kolka, R. K. *SPRUCE Peat Physical and Chemical Characteristics from Experimental Plot Cores, 2012*; Carbon Dioxide Inf. Anal. Center, Oak Ridge Natl. Lab. U.S. Dep. Energy: Oak Ridge, Tennessee, U.S.A., 2014.
- (48) Graham, J. D.; Glenn, N. F.; Spaete, L. P.; Hanson, P. J. Characterizing Peatland Microtopography Using Gradient and Microform-Based Approaches. *Ecosystems* **2020**, *23*, 1464–1480.
- (49) Hassel, K.; Kyrkjæide, M. O.; Yousefi, N.; Prestø, T.; Stenøien, H. K.; Shaw, J. A.; Flatberg, K. I. *Sphagnum Divinum* (Sp. Nov.) and S. Medium Limpr. and Their Relationship to S. Magellanicum Brid. *J. Bryolog.* **2018**, *40*, 197–222.
- (50) Hanson, P. J.; Riggs, J. S.; Nettles, W. R.; Phillips, J. R.; Krassovski, M. B.; Hook, L. A.; Gu, L.; Richardson, A. D.; Aubrecht, D. M.; Ricciuto, D. M.; Warren, J. M.; Barbier, C. Attaining Whole-Ecosystem Warming Using Air and Deep-Soil Heating Methods with an Elevated CO₂ Atmosphere. *Biogeosciences* **2017**, *14*, 861–883.
- (51) Griffiths, N. A.; Sebestyen, S. D. *SPRUCE Porewater Chemistry Data for Experimental Plots Beginning in 2013*; Carbon Dioxide Inf. Anal. Center, Oak Ridge Natl. Lab. U.S. Dep. Energy: Oak Ridge, TN, 2016; Vol. 1–15.
- (52) Ravel, B.; Newville, M. ATHENA, ARTEMIS, HEPHAESTUS: Data Analysis for X-Ray Absorption Spectroscopy Using IFEFFIT. *J. Synchrotron Radiat.* **2005**, *12*, 537–541.
- (53) Nicholas, S. L.; Erickson, M. L.; Woodruff, L. G.; Knaeble, A. R.; Marcus, M. A.; Lynch, J. K.; Toner, B. M. Solid-Phase Arsenic Speciation in Aquifer Sediments: A Micro-X-Ray Absorption Spectroscopy Approach for Quantifying Trace-Level Speciation. *Geochim. Cosmochim. Acta* **2017**, *211*, 228–255.
- (54) Cron, B. R.; Sheik, C. S.; Kafantaris, F.-C. A.; Druschel, G. K.; Seewald, J. S.; German, C. R.; Dick, G. J.; Breier, J. A.; Toner, B. M. Dynamic Biogeochemistry of the Particulate Sulfur Pool in a Buoyant Deep-Sea Hydrothermal Plume. *ACS Earth Space Chem.* **2020**, *4*, 168–182.
- (55) Zeng, T.; Arnold, W. A.; Toner, B. M. Microscale Characterization of Sulfur Speciation in Lake Sediments. *Environ. Sci. Technol.* **2013**, *47*, 1287–1296.
- (56) Manceau, A.; Nagy, K. L. Quantitative Analysis of Sulfur Functional Groups in Natural Organic Matter by XANES Spectroscopy. *Geochim. Cosmochim. Acta* **2012**, *99*, 206–223.
- (57) Burton, E. D.; Bush, R. T.; Sullivan, L. A.; Hocking, R. K.; Mitchell, D. R. G.; Johnston, S. G.; Fitzpatrick, R. W.; Raven, M.; McClure, S.; Jang, L. Y. Iron-Monosulfide Oxidation in Natural Sediments: Resolving Microbially Mediated S Transformations Using XANES, Electron Microscopy, and Selective Extractions. *Environ. Sci. Technol.* **2009**, *43*, 3128–3134.
- (58) Behyan, S.; Hu, Y.; Urquhart, S. G. Sulfur 1 s near Edge X-Ray Absorption Fine Structure Spectroscopy of Thiophenic and Aromatic Thioether Compounds. *J. Chem. Phys.* **2013**, *138*, 214302.
- (59) 4500-S2-D Methylene Blue Method <http://standardmethods.org/> (accessed 2021-03-29).
- (60) APHA. *Standard Methods for the Examination of Water and Wastewater*, 23rd ed.; American Public Health Association: Washington DC, USA, 2017.
- (61) U.S. Environmental Protection Agency. *Method 1631, Revision E: Mercury in Water by Oxidation, Purge and Trap, and Cold Vapor Atomic Fluorescence Spectrometry*, 2002; pp 1–46. EPA 821-R-96-012.
- (62) U.S. Environmental Protection Agency. *Method 1630, Methyl Mercury in Water by Distillation, Aqueous Ethylation, Purge and Trap, and Cold-Vapor Atomic Fluorescence Spectrometry*, 1998; pp 1–46. EPA-821-R-01-020.
- (63) Hintelmann, H.; Ogrinc, N. Determination of Stable Mercury Isotopes by ICP/MS and Their Application in Environmental Studies. *Biogeochemistry of Environmentally Important Trace Elements*; American Chemical Society: Washington DC, USA, 2003; pp 321–338.
- (64) Hintelmann, H.; Evans, R. D.; Villeneuve, J. Y. Measurement of Mercury Methylation in Sediments by Using Enriched Stable Mercury Isotopes Combined with Methylmercury Determination by Gas Chromatography-Inductively Coupled Plasma Mass Spectrometry. *J. Anal. At. Spectrom.* **1995**, *10*, 619–624.
- (65) Lehnher, I.; Emmerton, C. A.; Barker, J. D.; Kirk, J. L. Methylmercury Cycling in High Arctic Wetland Ponds: Sources and Sinks. *Environ. Sci. Technol.* **2012**, *46*, 10514–10522.
- (66) Gionfriddo, C. M.; Wymore, A. M.; Jones, D. S.; Wilpiseski, R. L.; Lynes, M. M.; Christensen, G. A.; Soren, A.; Gilmour, C. C.; Podar, M.; Elias, D. A. An Improved HgCAB Primer Set and Direct High-Throughput Sequencing Expand Hg-Methylator Diversity in Nature. *Front. Microbiol.* **2020**, *11*, 541554.

- (67) R Core Team. *R: A Language and Environment for Statistical Computing*; R Foundation for Statistical Computing: Vienna, Austria, 2017.
- (68) de Mendiburu, F.; Yaseen, M. *Agricolae: Statistical Procedures for Agricultural Research*, 2020.
- (69) Steel, R. G. D.; Torrie, J. H.; Dickey, D. A. *Principles and Procedures of Statistic a Biometrical Approach*, 3rd ed.; The McGraw Hill Companies, Inc., 1997.
- (70) Skjellberg, U.; Qian, J.; Frech, W.; Xia, K.; Bleam, W. F. Distribution of Mercury, Methyl Mercury and Organic Sulphur Species in Soil, Soil Solution and Stream of a Boreal Forest Catchment. *Biogeochemistry* **2003**, *64*, 53–76.
- (71) Novák, M.; Buzek, F.; Adamova, M. Vertical Trends in 13C, 15N and 34S Ratios in Bulk Sphagnum Peat. *Soil Biol. Biochem.* **1999**, *31*, 1343–1346.
- (72) Vile, M. A.; Novak, M. Sulfur Cycling in Boreal Peatlands: From Acid Rain to Global Climate Change. *Boreal Peatland Ecosystems*; Springer Berlin Heidelberg, 2006.
- (73) McCarter, C. P. R.; Branfireun, B. A.; Price, J. S. Nutrient and Mercury Transport in a Sub-Arctic Ladder Fen Peatland Subjected to Simulated Wastewater Discharges. *Sci. Total Environ.* **2017**, *609*, 1349–1360.
- (74) Wang, B.; Nilsson, M. B.; Eklöf, K.; Hu, H.; Ehnvall, B.; Bravo, A. G.; Zhong, S.; Åkeblom, S.; Björn, E.; Bertilsson, S.; Skjellberg, U.; Bishop, K. Opposing Spatial Trends in Methylmercury and Total Mercury along a Peatland Chronosequence Trophic Gradient. *Sci. Total Environ.* **2020**, *718*, 137306.
- (75) Benoit, J. M.; Fitzgerald, W. F.; Damman, A. W. H. The Biogeochemistry of an Ombrotrophic Bog: Evaluation of Use as an Archive of Atmospheric Mercury Deposition. *Environ. Res.* **1998**, *78*, 118–133.
- (76) Fissore, C.; Nater, E. A.; McFarlane, K. J.; Klein, A. S. Decadal Carbon Decomposition Dynamics in Three Peatlands in Northern Minnesota. *Biogeochemistry* **2019**, *145*, 63–79.
- (77) Givélet, N.; Roos-Barraclough, F.; Shoty, W. Predominant Anthropogenic Sources and Rates of Atmospheric Mercury Accumulation in Southern Ontario Recorded by Peat Cores from Three Bogs: Comparison with Natural “Background” Values (Past 8000 Years). *J. Environ. Monit.* **2003**, *5*, 935–949.
- (78) Christensen, G. A.; Gionfriddo, C. M.; King, A. J.; Moberly, J. G.; Miller, C. L.; Somenahally, A. C.; Callister, S. J.; Brewer, H.; Podar, M.; Brown, S. D.; Palumbo, A. V.; Brandt, C. C.; Wymore, A. M.; Brooks, S. C.; Hwang, C.; Fields, M. W.; Wall, J. D.; Gilmour, C. C.; Elias, D. A. Determining the Reliability of Measuring Mercury Cycling Gene Abundance with Correlations with Mercury and Methylmercury Concentrations. *Environ. Sci. Technol.* **2019**, *53*, 8649–8663.
- (79) Santelmann, M. V. Cellulose Mass Loss in Ombrotrophic Bogs of Northeastern North America. *Can. J. Bot.* **1992**, *70*, 2378–2383.
- (80) Branfireun, B. A. Does Microtopography Influence Subsurface Porewater Chemistry? Implications for the Study of Methylmercury in Peatlands. *Wetlands* **2004**, *24*, 207–211.
- (81) Mandernack, K. W.; Lynch, L.; Krouse, H. R.; Morgan, M. D. Sulfur Cycling in Wetland Peat of the New Jersey Pinelands and Its Effect on Stream Water Chemistry. *Geochim. Cosmochim. Acta* **2000**, *64*, 3949–3964.
- (82) Einsiedl, F.; Mayer, B.; Schäfer, T. Evidence for Incorporation of H₂S in Groundwater Fulvic Acids from Stable Isotope Ratios and Sulfur K-Edge X-Ray Absorption Near Edge Structure Spectroscopy. *Environ. Sci. Technol.* **2008**, *42*, 2439–2444.
- (83) Heitmann, T.; Blodau, C. Oxidation and Incorporation of Hydrogen Sulfide by Dissolved Organic Matter. *Chem. Geol.* **2006**, *235*, 12–20.
- (84) Hoffmann, M.; Mikutta, C.; Kretzschmar, R. Bisulfide Reaction with Natural Organic Matter Enhances Arsenite Sorption: Insights from X-Ray Absorption Spectroscopy. *Environ. Sci. Technol.* **2012**, *46*, 11788–11797.
- (85) Novák, M.; Bottrell, S. H.; Přečková, E. Sulfur Isotope Inventories of Atmospheric Deposition, Spruce Forest Floor and Living Sphagnum along a NW-SE Transect across Europe. *Biogeochemistry* **2001**, *53*, 23–50.
- (86) Lin, X.; Tfaily, M. M.; Green, S. J.; Steinweg, J. M.; Chanton, P.; Invittaya, A.; Chanton, J. P.; Cooper, W.; Schadt, C.; Kostka, J. E. Microbial Metabolic Potential for Carbon Degradation and Nutrient (Nitrogen and Phosphorus) Acquisition in an Ombrotrophic Peatland. *Am. Soc. Microbiol.* **2014**, *80*, 3531–3540.
- (87) Lin, X.; Tfaily, M. M.; Steinweg, J. M.; Chanton, P.; Esson, K.; Yang, Z. K.; Chanton, J. P.; Cooper, W.; Schadt, C. W.; Kostka, J. E. Microbial Community Stratification Linked to Utilization of Carbohydrates and Phosphorus Limitation in a Boreal Peatland at Marcel Experimental Forest, Minnesota, USA. *Am. Soc. Microbiol.* **2014**, *80*, 3518–3530.
- (88) Lu, X.; Gu, W.; Zhao, L.; Ul Haque, M. F.; DiSpirito, A. A.; Semrau, J. D.; Gu, B. Methylmercury Uptake and Degradation by Methanotrophs. *Sci. Adv.* **2017**, *3*, No. e1700041.
- (89) Zhao, L.; Chen, H.; Lu, X.; Lin, H.; Christensen, G. A.; Pierce, E. M.; Gu, B. Contrasting Effects of Dissolved Organic Matter on Mercury Methylation by *Geobacter Sulfurreducens* PCA and *Desulfovibrio Desulfuricans* ND132. *Environ. Sci. Technol.* **2017**, *51*, 10468–10475.
- (90) Liem-Nguyen, V.; Skjellberg, U.; Björn, E. Thermodynamic Modeling of the Solubility and Chemical Speciation of Mercury and Methylmercury Driven by Organic Thiols and Micromolar Sulfide Concentrations in Boreal Wetland Soils. *Environ. Sci. Technol.* **2017**, *51*, 3678–3686.
- (91) Skjellberg, U.; Bloom, P. R.; Qian, J.; Lin, C.-M.; Bleam, W. F. Complexation of Mercury(II) in Soil Organic Matter: EXAFS Evidence for Linear Two-Coordination with Reduced Sulfur Groups. *Environ. Sci. Technol.* **2006**, *40*, 4174–4180.
- (92) Yoon, S.-J.; Diener, L. M.; Bloom, P. R.; Nater, E. A.; Bleam, W. F. X-Ray Absorption Studies of CH₃Hg⁺-Binding Sites in Humic Substances. *Geochim. Cosmochim. Acta* **2005**, *69*, 1111–1121.
- (93) Liu, Y.-R.; Lu, X.; Zhao, L.; An, J.; He, J.-Z.; Pierce, E. M.; Johs, A.; Gu, B. Effects of Cellular Sorption on Mercury Bioavailability and Methylmercury Production by *Desulfovibrio Desulfuricans* ND132. *Environ. Sci. Technol.* **2016**, *50*, 13335–13341.
- (94) Graham, A. M.; Bullock, A. L.; Maizel, A. C.; Elias, D. A.; Gilmour, C. C. Detailed Assessment of the Kinetics of Hg-Cell Association, Hg Methylation, and Methylmercury Degradation in Several *Desulfovibrio* Species. *Appl. Environ. Microbiol.* **2012**, *78*, 7337–7346.
- (95) Schaefer, J. K.; Rocks, S. S.; Zheng, W.; Liang, L.; Gu, B.; Morel, F. M. M. Active Transport, Substrate Specificity, and Methylation of Hg(II) in Anaerobic Bacteria. *Proc. Natl. Acad. Sci.* **2011**, *108*, 8714–8719.
- (96) Lin, H.; Lu, X.; Liang, L.; Gu, B. Cysteine Inhibits Mercury Methylation by *Geobacter Sulfurreducens* PCA Mutant Δomc-BESTZ. *Environ. Sci. Technol. Lett.* **2015**, *2*, 144–148.
- (97) Liem-Nguyen, V.; Skjellberg, U.; Björn, E. Methylmercury Formation in Boreal Wetlands in Relation to Chemical Speciation of Mercury(II) and Concentration of Low Molecular Mass Thiols. *Sci. Total Environ.* **2021**, *755*, 142666.
- (98) Sebestyen, S. D.; Verry, E. S.; Elling, A. E.; Kyllander, R. L.; Roman, D. T.; Burdick, J. M.; Lany, N. K.; Kolka, R. K. *Marcell Experimental Forest Peatland and Upland Water Table Elevations*, 2nd ed.; Forest Service Research Data Archive: Fort Collins, CO, USA, 2021.
- (99) Jonsson, S.; Skjellberg, U.; Nilsson, M. B.; Westlund, P.-O.; Shchukarev, A.; Lundberg, E.; Björn, E. Mercury Methylation Rates for Geochemically Relevant Hg(II) Species in Sediments. *Environ. Sci. Technol.* **2012**, *46*, 11653–11659.
- (100) Hammerschmidt, C. R.; Fitzgerald, W. F. Geochemical Controls on the Production and Distribution of Methylmercury in Near-Shore Marine Sediments. *Environ. Sci. Technol.* **2004**, *38*, 1487–1495.
- (101) Lie, T. J.; Pitta, T.; Leadbetter, E. R.; Godchaux, W.; Leadbetter, J. R. Sulfonates: Novel Electron Acceptors in Anaerobic Respiration. *Arch. Microbiol.* **1996**, *166*, 204–210.

(102) Lie, T. J.; Leadbetter, J. R.; Leadbetter, E. R. Metabolism of Sulfonic Acids and Other Organosulfur Compounds by Sulfate-Reducing Bacteria. *Geomicrobiol. J.* **1998**, *15*, 135–149.

(103) Visscher, P. T.; Gritzer, R. F.; Leadbetter, E. R. Low-Molecular-Weight Sulfonates, a Major Substrate for Sulfate Reducers in Marine Microbial Mats. *Appl. Environ. Microbiol.* **1999**, *65*, 3272–3278.

(104) Solomon, D.; Lehmann, J.; Zarruk, K. K. De; Dathe, J.; Kinyangi, J.; Liang, B.; Machado, S. Speciation and Long- and Short-Term Molecular-Level Dynamics of Soil Organic Sulfur Studied by X-Ray Absorption Near-Edge Structure Spectroscopy. *J. Environ. Qual.* **2011**, *40*, 704.

(105) Zhao, F.; Lehmann, J.; Solomon, D.; Fox, M.; McGrath, S. Sulphur Speciation and Turnover in Soils: Evidence from Sulphur K-Edge XANES Spectroscopy and Isotope Dilution Studies. *Soil Biol. Biochem.* **2006**, *38*, 1000–1007.

(106) Solomon, D.; Lehmann, J.; Kinyangi, J.; Pell, A.; Theis, J.; Riha, S.; Ngoze, S.; Amelung, W.; Preez, C.; Machado, S.; Ellert, B.; Janzen, H. Anthropogenic and Climate Influences on Biogeochemical Dynamics and Molecular-Level Speciation of Soil Sulfur. *Ecol. Appl.* **2009**, *19*, 989–1002.

(107) Churka Blum, S.; Lehmann, J.; Solomon, D.; Caires, E. F.; Alleoni, L. R. F.; Alleoni, F. Sulfur Forms in Organic Substrates Affecting S Mineralization in Soil. *Geoderma* **2013**, *200–201*, 156–164.

(108) Friedrich, C. G.; Rother, D.; Bardischewsky, F.; Quentmeier, A.; Fischer, J. Oxidation of Reduced Inorganic Sulfur Compounds by Bacteria: Emergence of a Common Mechanism? *Appl. Environ. Microbiol.* **2001**, *67*, 2873–2882.

(109) Luther, G. W.; Findlay, A. J.; Macdonald, D. J.; Owings, S. M.; Hanson, T. E.; Beinart, R. A.; Girguis, P. R. Thermodynamics and Kinetics of Sulfide Oxidation by Oxygen: A Look at Inorganically Controlled Reactions and Biologically Mediated Processes in the Environment. *Front. Microbiol.* **2011**, *2*, 62.

(110) Feng, S.; Ai, Z.; Zheng, S.; Gu, B. Effects of Dryout and Inflow Water Quality on Mercury Methylation in a Constructed Wetland. *Water, Air, Soil Pollut.* **2014**, *225*, 1929.

(111) Munthe, J.; Bodaly, R. A.; Branfireun, B. A.; Driscoll, C. T.; Gilmour, C. C.; Harris, R.; Horvat, M.; Lucotte, M.; Malm, O. Recovery of Mercury-Contaminated Fisheries. *J. Hum. Environ.* **2007**, *36*, 33–44.

**HAZARD AWARENESS
REDUCES LAB INCIDENTS**

**ACS Essentials of
Lab Safety for
General Chemistry**

A new course from the
American Chemical Society

ACS Institute
Learn. Develop. Excel.

EXPLORE
ORGANIZATIONAL
SALES
solutions.acs.org/essentialsoflabsafety

REGISTER FOR
INDIVIDUAL ACCESS
institute.acs.org/courses/essentials-lab-safety.html

Supplemental Information

THE ROLE OF ESTER SULFATE AND ORGANIC DISULFIDE IN MERCURY METHYLATION IN PEATLAND SOILS

Caroline E. Pierce^a, *Olha S. Furman*^{ab}, *Sarah L. Nicholas*^{ac}, *Jill Coleman Wasik*^d, *Caitlin M. Gionfriddo*^{ef}, *Ann M. Wymore*^e, *Stephen D. Sebestyen*^g, *Randall K. Kolka*^g, *Carl P.J. Mitchell*^h, *Natalie A. Griffiths*ⁱ, *Dwayne A. Elias*^e, *Edward A. Nater*^a, and *Brandy M. Toner*^{a*}

^a Department of Soil, Water, and Climate, University of Minnesota, St. Paul, MN 55108 USA

^b Current affiliation: Department of Agriculture, Water, and the Environment, Australian Government, Canberra, Australia

^c Current affiliation: Brookhaven National Laboratory - National Synchrotron Light Source II, Upton, NY 11973 USA

^d Plant and Earth Science Department, University of Wisconsin River Falls, River Falls, WI 54022 USA

^e Biosciences Division, Oak Ridge National Laboratory, Oak Ridge, TN 37831 USA

^f Current affiliation: Smithsonian Environmental Research Center, Edgewater, MD 21037 USA

^g USDA Forest Service, Northern Research Station, Grand Rapids, MN 55744 USA

^h Department of Physical and Environmental Sciences, University of Toronto Scarborough, Scarborough, ON Canada

ⁱ Environmental Sciences Division, Oak Ridge National Laboratory, Oak Ridge, TN 37831 USA

*Corresponding author email: toner@umn.edu

Table of Contents

Impact of Water Table Height.....	S1
Detailed Methods	
2.2 Sampling Methods.....	S2
2.3 Sulfur Concentration and Speciation in Peatland Soil.....	S3
2.4 Acid Volatile Sulfur and Sulfate in Porewaters.....	S4
2.5 Total Mercury and MeHg Concentration in Peatland Soil.....	S5
2.6 Instantaneous mercury methylation and demethylation rate constants.....	S5
2.7 <i>hgcAB</i> Primer Sequencing.....	S6
Figure S1.....	S8
Figure S2.....	S8
Figure S3.....	S9
Figure S4.....	S10
Figure S5.....	S10
Figure S6.....	S11
Figure S7.....	S11
Figure S8.....	S12
Table S1.....	S13
Table S2.....	S14
Table S3.....	S15
Table S4.....	S16
Table S5.....	S17
Table S6.....	S18
Table S7.....	S19
Table S8.....	S20
Table S9.....	S20
References.....	S21

1 **Impact of Water Table Height**

2 The water table is critical in determining how much MeHg is produced and exported from
3 peatlands. When the water table is high, more MeHg is produced and there is more lateral runoff
4 leaving the peatland and entering the downstream surface waters. When the water table is low,
5 MeHg continues to be produced and there is little or no direct export from the peatland to surface
6 waters. Re-wetting events are also important because MeHg is released as a surge during the re-
7 wetting event. The porewater mercury concentrations would respond more quickly to changes in
8 the water table than peat mercury concentrations.

9 Recent articles by Haynes et al. have directly investigated the impacts of changing water tables
10 on porewater mercury, gaseous mercury, and peat mercury ¹⁻³.

- 11 • Porewater: Lower and more variable water table regimes increase both THg and MeHg
12 concentrations in peat porewater. These differences are related to greater peat
13 decomposition and internal renewal of electron acceptors ¹.
- 14 • Gaseous: Re-wetting of peat following extended water table drawdown may increase
15 gaseous mercury fluxes. Once saturated, emission of mercury to the atmosphere may be
16 inhibited ².
- 17 • Solid peat: Peat THg and MeHg concentrations increased significantly within the
18 mesotelm when water tables were lowered. Increased desorption of Hg(II) and MeHg
19 from the solid phase peat into porewater occurred with a lowered water table, likely due
20 to enhanced aerobic peat decomposition. Deeper, more variable water tables coincided
21 with increased MeHg accumulation within the mesotelm. Persistent high water tables
22 promoted the net downward movement of Hg(II) and MeHg ³.

23 These studies by Haynes et al. involved an experiment where the water table was experimentally
24 changed over 20 cm. However, over the course of 1998 to 2012, including prolonged droughts
25 during 2006 and 2007, the water table in the S1 bog had a maximum elevation change of 94 cm.
26 This means the findings in Haynes et al. might be even more amplified in our field site.

27 **Detailed Methods**

28 **2.2 Sampling Methods**

29 Peat cores were collected to a depth of -200 cm from six locations in triplicate for a total of 18
30 cores in August 2012. Three cores were obtained within close proximity and composited
31 according to depth. A total of 164 samples were collected. A 7.5 cm stainless steel drill (rotary)
32 corer was used to collect surface samples (0 to -30 cm)⁴. Deeper peat cores were collected with
33 a Russian peat corer⁵ from hummock and hollow surfaces to depths of 200 cm. Depths -30 cm to
34 -50 cm were divided in 10 cm increments and depths -50 cm to -200 cm were divided in 25 cm
35 increments⁴. All depths were reported with respect to hollow surfaces (0 cm); negative values
36 indicate depths below the hollow surface elevation, while positive values indicate depths within
37 hummocks and above the hollow surface. Subsamples were immediately taken for sulfur and
38 mercury analyses. Subsamples for sulfur analyses were processed in a glove-bag in the field and
39 stored in argon filled mylar pouches containing Anaeropak oxygen scrubbers (R681001,
40 Mitsubishi Gas Chemical Co., Tokyo, Japan) in a freezer to prevent oxidative changes to the
41 samples. All samples for sulfur were protected from ambient oxygen during sample shipping,
42 storage, and analysis. Subsamples for mercury analyses were stored frozen until freeze-dried for
43 further analysis.

44 Porewaters were collected in October 2013 from six piezometer nests located near the location of
45 the collected cores⁶. The day before sampling, all water was removed from the piezometers and

46 the headspace was purged with argon. On the day of sampling the porewaters had refilled the
47 piezometers while still overlaid with argon. The porewaters were pumped via acid-washed
48 peristaltic pump tubing connected to a hypodermic needle through a luer-lock adapter into pre-
49 evacuated serum bottles filled with nitrogen. Piezometers were made from 5 cm diameter
50 polyvinyl chloride (PVC) pipe and were screened with 0.25 mm slots every 1 cm over 10 cm
51 intervals. The top of the screened interval was placed at 0, -30, -50, and -100 cm depths.

52 **2.3 Sulfur Concentration and Speciation in Peatland Soil**

53 Peat and *Sphagnum* subsamples (*S. divinum* and *S. angustifolium/fallax*) collected from surface
54 and subsurface layers were dried in a Bel-art gas purge box flushed with argon or nitrogen
55 continuously for 3 - 4 days. Dried peat and *Sphagnum* samples were homogenized under liquid
56 nitrogen using a ceramic mortar and pestle in a portable Captair pyramid glovebox, split for
57 elemental analysis and sulfur 1s X-ray absorption near edge structure (XANES) spectroscopy,
58 and sealed in argon filled mylar pouches containing Anaeropack oxygen scrubbers before further
59 analyses. The purpose of measuring sulfur XANES in *Sphagnum* was to measure the sulfur
60 chemistry from living biomass input.

61 At the SXRMB beamline, ground samples were applied on a low-sulfur double-adhesive carbon
62 tape and attached to a copper multi-sample plate in a portable glove-bag filled with argon under
63 positive gas pressure. At the 9-BM beamline, a stainless-steel pelletizer was used to form peat
64 pellets which were deposited on a double-adhesive carbon tape attached to a sample holder. At
65 both beamlines, the prepped samples were sealed in a mylar bag until placed into the sample
66 chamber under a helium atmosphere or vacuum for analysis with fluorescence detection.
67 Replicate analyses demonstrated that XANES spectra were reproducible in helium and vacuum.

68 At both SXRMB and 9-BM beamlines, photon damage to the samples was not observed and each
69 spectrum was the average of two to three scans per sample. Energy calibration of the
70 monochromator was performed using gypsum (CaSO_4) with the absorption maximum set to a
71 value of 2482.74 eV.

72 Sulfur XANES spectra were energy calibrated, averaged, pre-edge subtracted, and post-edge
73 normalized in *Athena*⁷. Sulfur XANES spectra were analyzed by linear combination fitting
74 (LCF) with reference spectra using *mrfitty*⁸. Linear combination fitting results in a description of
75 each experimental spectrum as a proportion of reference spectra on a per atom basis. The
76 appearance of a reference spectrum, for example, sodium dodecyl sulfate (SDS), in the final best
77 fit does not indicate that SDS is in the sample. Rather, it indicates that the sulfur in the sample
78 has a bonding, coordination, and valence state similar to the sulfur in the reference material.
79 Therefore, LCF results are binned to translate from specific reference spectra (e.g., SDS) to the
80 sulfur species it represents (e.g., ester sulfate) (Table S4 and S5). For environmental samples, the
81 quality of the fit depends on the degree to which the reference spectra are representative of the
82 chemistry of the field site.

83 **2.4 Acid Volatile Sulfur and Sulfate in Porewaters**

84 Porewaters were pumped into 50 ml serum bottles loaded with 1N Zn-acetate and concentrated
85 NaOH in a pure nitrogen environment and kept refrigerated for acid volatile sulfur analysis. A
86 measured amount of sample was acidified with HCl in an extraction vessel; all acid-extractable
87 sulfides in the sample were protonated to form H_2S . The H_2S was flushed from the extraction jar
88 by oxygen-free N_2 gas into a trapping vial containing 0.25 M NaOH trapping solution. The
89 methylene blue colorimetric method⁹ was used for sulfide analysis through the reaction of H_2S

90 and dimethyl-p-phenylenediamine in the presence of ferric iron in an acidic matrix. Solution
91 absorbance was measured at 660 nm on a Lachat QuikChem 8000 Autoanalyzer Lachat ¹⁰.
92 Standards were created from a stock saturated sodium sulfide solution. The concentration of the
93 stock was determined by diluting an aliquot of stock solution in sulfide antioxidizing buffer and
94 then titrating to the endpoint with 0.1 M lead perchlorate solution. An Orion silver/sulfide
95 electrode was used to measure the titration. Standards and samples were analyzed within minutes
96 of creation.

97 **2.5 Total Mercury and MeHg Concentration in Peatland Soil**

98 Prior to THg analysis, freeze-dried peat samples were digested in concentrated nitric acid
99 overnight at 70 °C ^{11,12}. Prior to MeHg analysis, separate freeze-dried peat subsamples were
100 digested in potassium hydroxide/methanol for 4 hours at 90 °C ¹³. Ten percent of samples
101 analyzed for THg or MeHg were run in duplicate or spiked with known amounts of THg or
102 MeHg (respectively). In addition, blanks and standard reference material were run every ~15
103 samples.

104 **2.6 Instantaneous mercury methylation and demethylation rate constants**

105 Samples for instantaneous methylation/demethylation rates were collected in 2016 from the S1
106 bog. Using the same approach as outlined in Mitchell and Gilmour (2008) ¹⁴, peat was incubated
107 with simultaneous additions of enriched-abundance ²⁰⁰Hg²⁺ (94.3%) and Me²⁰¹Hg⁺ (84.7%; both
108 isotopes from Trace Science International) and analyzed for the production or degradation of
109 labelled MeHg to assess potential methylation and demethylation rates constants, respectively.
110 Peat was incubated in clear polycarbonate 5 cm diameter core tubes in the dark at 19 °C for 16
111 hours. Incubations were finalized by extruding the top 30 cm at 5 cm intervals and then 10 cm

112 intervals for the remainder of the core (to -50 cm), and then immediately freezing the samples.
113 Peat samples were freeze-dried and homogenized before analysis.

114 For MeHg analysis, samples were distilled and then analyzed by isotope dilution – gas
115 chromatography – inductively couple plasma mass spectrometry (ID-GC-ICPMS), as established
116 by Hintelmann (1997) ¹⁵ and recently described in Haynes et al. (2019) ³. Concentrations of both
117 ambient and Me^{20x}Hg concentrations in excess of natural abundance were obtained from the
118 same sample according to the isotope dilution calculations of Hintelmann and Ogrinc (2003) ¹⁶.

119 For THg analysis, the peat samples were digested in at 70 °C nitric acid and analyzed per US
120 EPA Method 1631 ¹⁷ on a Tekran 2600 system, but hyphenated to the ICP-MS for detection of
121 isotopes. The initial concentrations of excess Me²⁰¹Hg were given as the value of excess T²⁰¹Hg
122 at the end of the incubation, given that the methylated mercury isotope was entirely MeHg.

123 **2.7 *hgcAB* Primer Sequencing**

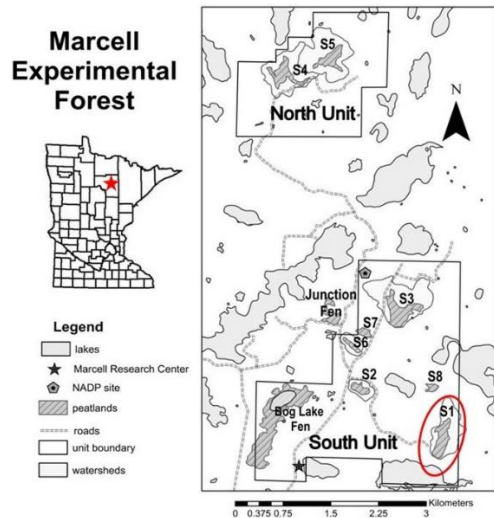
124 A total of 47 samples were collected from the S1 bog as described in section 2.2. Soil samples
125 were stored at –80 °C prior to DNA extraction. Genomic DNA (gDNA) was isolated from soils
126 using the MoBio Powersoil kit (now Qiagen DNeasy) with the addition of a 30-minute
127 incubation at 65 °C following the bead beating step.

128 For *hgcAB* amplification, 20 µL reaction mixtures contained 0.5 µM of primers ORNL-HgcAB-
129 uni-F (5' AAYGTCTGGTGYGCNGCVGG) and ORNL-HgcAB-uni-32R (5' CAG GCN CCG
130 CAY TCS ATR CA), Apex TaqRed polymerase (Genesee Scientific, San Diego, CA, United
131 States), and 0.5 ng µL⁻¹ (final concentration) gDNA template ¹⁸. A touch-down PCR protocol was
132 used with pre-incubation (2 minutes at 98 °C), then 5 cycles of denaturation (30 seconds at 98 °C),
133 annealing (30 seconds at 68 °C; –1 °C per cycle), and extension (30 seconds at 72 °C), then 30

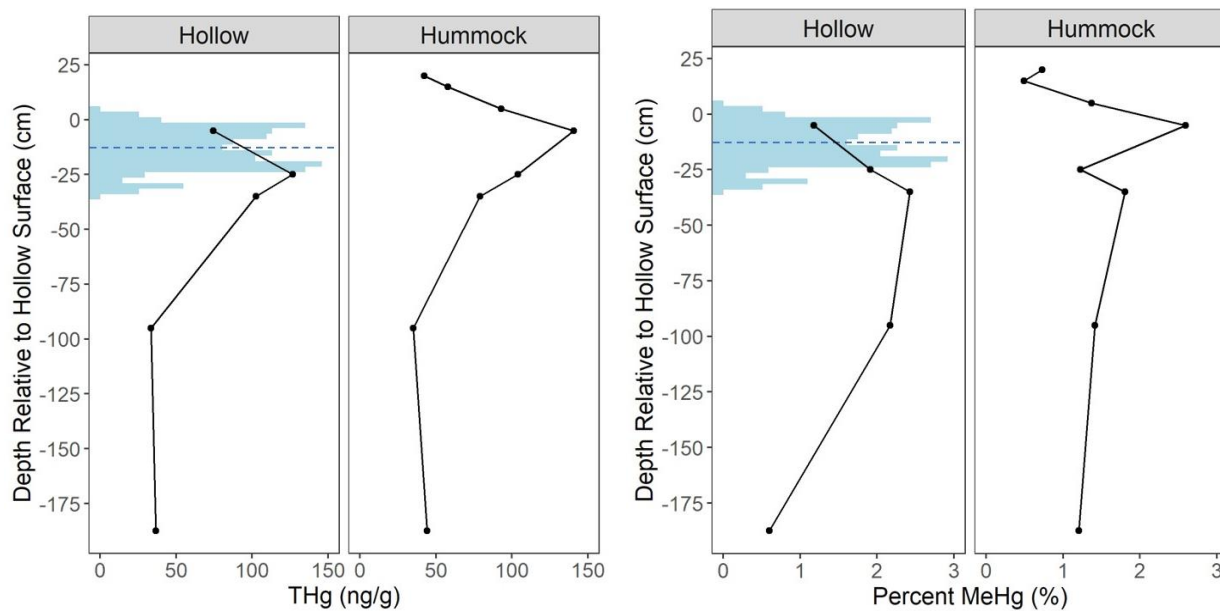
134 cycles of denaturation (30 seconds at 98 °C), annealing (30 seconds at 63 °C), and extension (60
135 seconds at 72 °C), then a final incubation step (2 minutes at 72 °C).

136 To create the clone libraries, *hgcAB* PCR products (~ 950 bp) from each sample were excised
137 from an 1% agarose gel, cleaned with Wizard SV Gel and PCR Clean-Up system (Promega,
138 Madison, WI, United States) and cloned into One Shot TOP10 cells with TOPO-TA cloning kit
139 (Invitrogen, Waltham, MA, United States). Cloned plasmids were screened for the ~ 1150 bp
140 insert using 100 pM of M13F (5' GTAAAACGACGGCCAG) and M13R (5'
141 CAGGAAACAGCTATGAC) primers with Apex TaqRed polymerase. The insert size was
142 confirmed (on 1% agarose gel), cleaned (Wizard SV Gel and PCR Clean-Up) and sent for Sanger
143 sequencing by Eurofins Genomics (Louisville, KY, United States). Approximately 5 clones were
144 chosen from each of the 47 sample libraries for sequencing, totaling 227 clones.

145 For classification of the clone sequences, the following pipeline was used. The *hgcAB* clone
146 sequences were trimmed of poor-quality bases and forward and reverse sequences aligned using
147 Geneious version 10.2. While both genes (*hgcA* and *hgcB*) were present in cloned sequences, only
148 the *hgcA* portion of the sequence was used for downstream analyses. Clone *hgcA* sequences were
149 trimmed to 654 nucleotide (nt) base pair (bp), corresponding to the 268 – 955 nt bp region of *hgcA*
150 in *Pseudodesulfovibrio mercurii* ND132 (previously *D. desulfuricans* ND132, Genbank
151 CP003220.1, 1150554:1151240)¹⁹. Clone *hgcA* sequences were clustered using 'cd-hit-est' on a
152 90 % sequence identity cut-off, then taxonomic classifications were assigned to operational
153 taxonomic units (OTU) using the ORNL HgcA reference package
154 'ORNL_HgcA_654_full.refpkg'^{18,20}. Taxonomic classifications of HgcA are based on
155 phylogenetic placement of translated HgcA sequences on a reference tree using 'pplacer' and
156 'guppy classify' with posterior probability classification cut-off of 90 %²¹.



158
 159 **Figure S1.** The map ²² showing the Marcell Experimental Forest in Minnesota, USA and six
 160 research catchments, including S1 (circled in red), within the MEF.

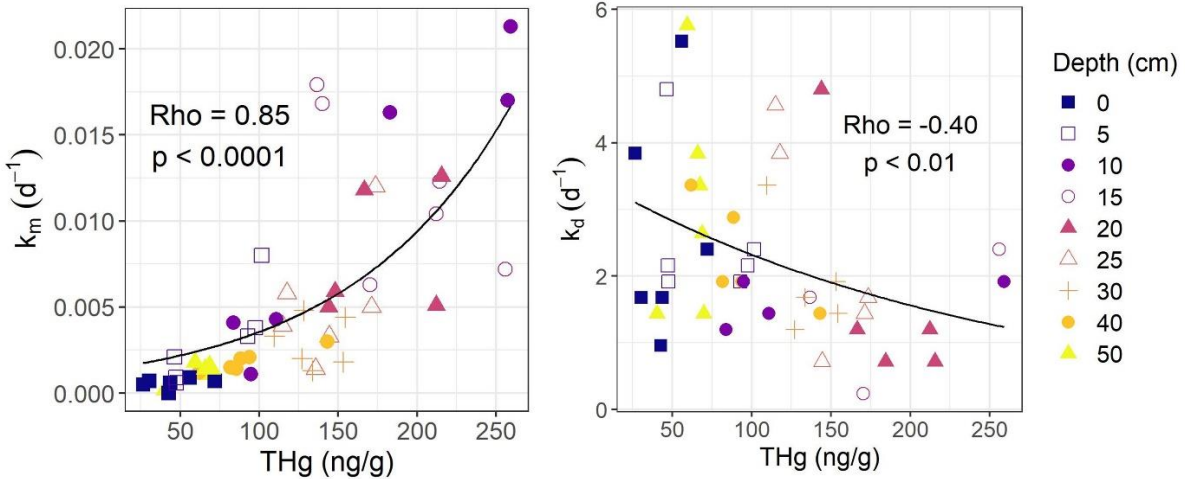


161
 162 **Figure S2.** Depth profiles - mean total mercury (THg) concentration and percent methylmercury
 163 in peatland soils for cores collected from hummocks and hollows. Blue shaded area is a
 164 histogram showing the range of daily water table positions (minimum: -35 cm, maximum: +6
 165 cm) in 2012. Blue dashed line is the water table height on the day of sampling.



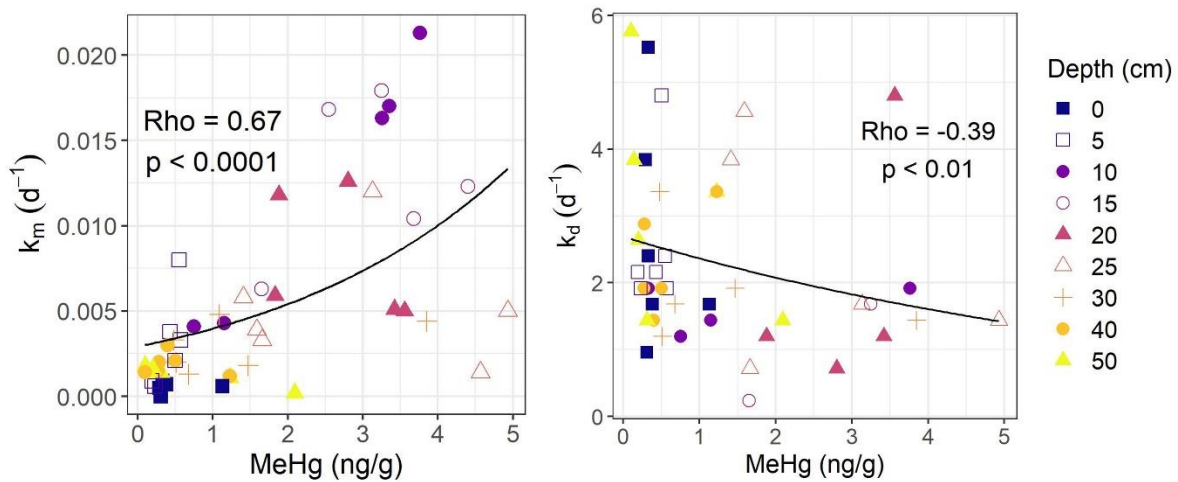
166

167 **Figure S3** *hgcAB* gene presence by binned group. Both *hgcA* and *hgcB* must be present but the
 168 taxonomy profile is based only on *hgcA*. *Geobacter* includes the genus *Geobacter* which uses
 169 iron as a terminal electron acceptor. *Methano-x* includes the genera *Methanolobus*,
 170 *Methanomicrobia*, *Methanoregula*, and *Methanosphaerula* which are methanogens. X-sulfuro-x
 171 includes the genera *Desulfuromonas* and *Desulfobacca* which use sulfate as a terminal electron
 172 acceptor. Other includes the genera *Auricularia*, *Bradyrhizobium*, *Dehalococcoides*,
 173 *Ethanoligenens*, *Granulicella*, *Koribacter*, *Microvirga*, *Pseudomonas*, *Rhodoplanes*, *Solibacter*,
 174 *Sulfuricella*, and *Vigna*. Uncultured are microbes that have not yet been cultured and
 175 characterized. In the hollows, *hgcAB* was not identified in depths 0 cm to -30 cm. At a depth of -
 176 100 cm the sampling interval increased, resulting in a wider spacing in the bars.



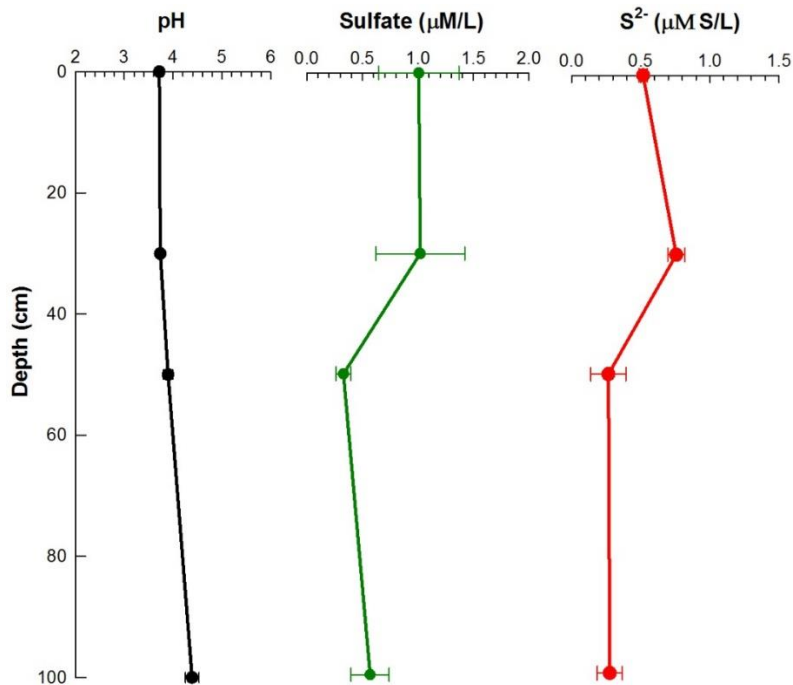
177

178 **Figure S4.** THg comparison plots of rate data from the S1 bog, August 2016. The left panel is
 179 the comparison of methylation rate constants to THg concentration and the right panel is the
 180 comparison with demethylation rate constants. The Spearman correlation coefficients are labeled
 181 as “Rho =” and the significance is listed below rho. All trends are significant ($p < 0.05$)



182

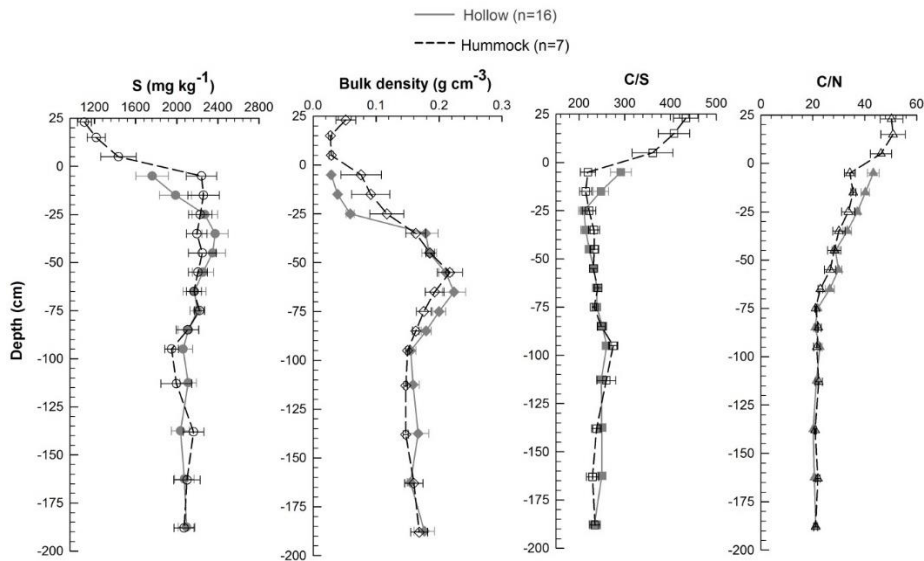
183 **Figure S5.** MeHg comparison plots of rate data from the S1 bog, August 2016. The left panel is
 184 the comparison of methylation rate constants to MeHg concentration and the right panel is the
 185 comparison with demethylation rate constants. The Spearman correlation coefficients are labeled
 186 as “Rho =” and the significance is listed below rho. All trends are significant ($p < 0.05$)



187

188 **Figure S6.** Depth profiles of mean porewater chemistry at the S1 bog, September 2013.

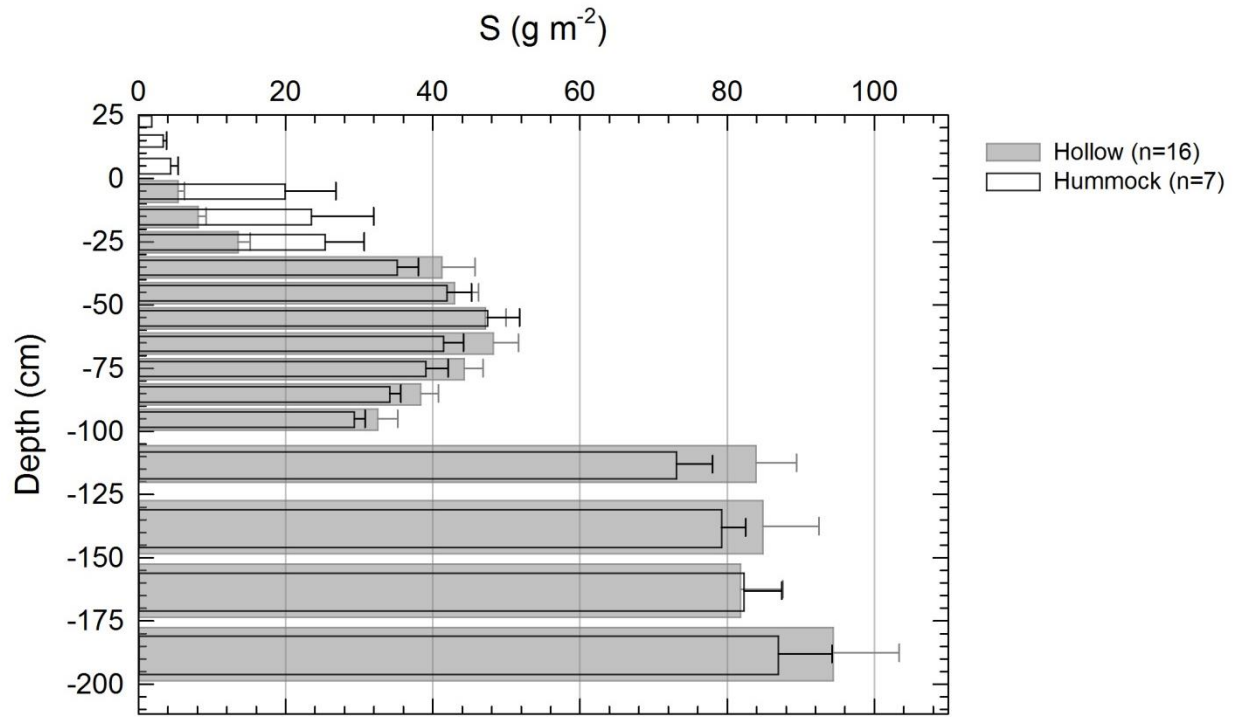
189 Piezometers are in hollow locations. Error bars are standard errors.



190

191 **Figure S7.** Depth profiles of total sulfur, bulk density, carbon:sulfur ratio (C/S), and

192 carbon:nitrogen ratio (C/N) in peat samples collected in 2012. Error bars are standard errors.



193

194 **Figure S8.** Depth profiles of sulfur stocks based on total sulfur and bulk density measurements
 195 in peat samples collected in 2012. Error bars are standard errors

196

197 **Table S1.** Complete list of sulfur reference compounds.

Reference Filename	Synchrotron Beamline	Compound	Species Bin Name	Sulfur-Bearing Moiety	Oxidation Index	Energy (eV)	Source
ANSA_ALS ^a	ALS-10.3.2	1-Amino-2-naphthol-4-sulfonic acid	Sulfonate	R-SO ₃ -H	+5	2481.31	e
Benzo_thiophene_YF_CLS ^b	CLS-SXRMB	Benzothiophene	Thiophene	Aromatic =R-S-R'	+1	2473.72	f
Bithiophene_YF_CLS	CLS-SXRMB	Bithiophene	Thiophene	Aromatic =R-S-R'	+1	2474.62	g
Cysteine_CLS_Tey_May_2015 ^c	CLS-SXRMB	Cysteine	Thiol	R-S-H	+0.2	2473.60	h
Cystine_APS_Tey ^d	APS-9BM	Cystine	Organic Disulfide	R-S-S-R'	-0.4	2472.75 / 2474.46	h
Gypsum_ALS_Tey	ALS-10.3.2	Gypsum	Inorganic Sulfate	CaSO ₄	+6	2482.69	e
Homocysteic_acid_ALS	ALS-10.3.2	Homocysteic acid	Sulfonate	R-SO ₃ -H	+5	2481.10	e
Methionine_CLS_Tey	CLS-SXRMB	Methionine	Organic Monosulfide	R-S-R'	+0.3	2473.60	h
Methionine_sulfoxide_CLS_Tey	CLS-SXRMB	Sulfoxide	Sulfoxide	R-S(=O)-R'	+2	2476.33	h
Saccharin_YF_CLS	CLS-SXRMB	Sulfonamide	Sulfone	R-SO ₂ -R'	+4	2480.02	g
SDS_CLS_Tey	CLS-SXRMB	Sodium dodecyl sulfate	Ester Sulfate	RO-S(=O) ₂ -O-	+6	2482.75	h
Sulfite_ALS	ALS-10.3.2	Sulfite	Sulfite	Na ₂ SO ₃ ²⁻	+4	2478.54 / 2482.14	e, i

a. Advanced Light Source (ALS) are measured in Total Electron Yield (TEY)

b. Canadian Light Source (CLS) are measured in TEY unless designated as "ambient"

c. Total Electron Yield (TEY) detection mode

d. Advanced Photon Source (APS)

e. Zeng et al. 2013

f. Behyan et al. 2013

g. Current article

h. Cron et al. 2020

i. Manceau and Nagy 2012

199 **Table S2.** Potential rate constant quality control and assurance measures

Ambient MeHg			Me ²⁰⁰ Hg		Me ²⁰¹ Hg	
Precision	Det. Limit	CRM recovery*	Precision	Det. Limit	Precision	Det. Limit
0.035	0.04 ng g ⁻¹	102 ± 5%	0.07	0.01 ng g ⁻¹	0.01	0.01 ng g ⁻¹

Ambient THg			T ²⁰⁰ Hg		T ²⁰¹ Hg	
Precision	Det. Limit	CRM recovery*	Precision	Det. Limit	Precision	Det. Limit
0.017	1.2 ng g ⁻¹	103 ± 5%	0.037	1.1 ng g ⁻¹	0.051	0.2 ng g ⁻¹

*CRM = certified reference material; ERM CC580 for MeHg, MESS-3 for THg

200

201

202 **Table S3.** Hummocks - Proportions of sulfur species as calculated by linear combination fittings in living *Sphagnum* and peat profiles
 203 from cores collected in 2012. All values are reported at mol % on a per atom basis. Total oxidized sulfur is the sum of inorganic
 204 sulfate, ester sulfate, sulfone, sulfonate, and sulfoxide. Total reduced sulfur is the sum of thiol, organic monosulfide, thiophene, and
 205 organic disulfide.

Sample ID	Depth to midpoint (cm)	Inorganic Sulfate (%)	Ester Sulfate (%)	Sulfone & Sulfonate (%)	Sulfoxide (%)	Total Oxidized Sulfur (%)	Thiol & Organic Monosulfide & Thiophene (%)	Organic disulfide (%)	Total Reduced Sulfur (%)
<i>S. angustifolium</i> <i>/ fallax</i>	Top	0	10	33	0	43	36	15	51
<i>S. divinum</i>	Top	16	0	30	0	46	33	13	46
06_T_Hum	21	0	17	22	0	39	39	14	52
10_T_Hum	25	13	0	32	0	45	37	12	49
13_T_Hum	25	0	21	14	11	46	46	0	46
Average		4	13	23	4	43	41	9	49
06_T_Hum	15	0	34	0	12	46	32	17	49
10_T_Hum	15	0	23	20	14	56	37	0	37
13_T_Hum	15	0	21	18	13	53	40	0	40
Average		0	26	13	13	52	37	6	42
06_T_Hum	5	0	33	0	12	45	33	19	52
10_T_Hum	5	0	16	21	0	37	36	23	59
13_T_Hum	5	0	18	22	0	40	36	16	52
Average		0	22	14	4	41	35	19	54
06_T_Hum	-5	0	12	16	0	29	37	27	64
10_T_Hum	-5	0	12	19	0	31	34	28	62
13_T_Hum	-5	0	13	20	0	33	35	27	61
Average		0	13	18	0	31	35	27	62
06_T_Hum	-25	0	16	20	0	35	34	25	59
10_T_Hum	-25	0	14	24	0	38	35	22	57
13_T_Hum	-25	0	0	22	0	22	48	25	73
Average		0	10	22	0	32	39	24	63
06_T_Hum	-35	0	11	20	0	32	39	24	63
10_T_Hum	-35	0	12	23	0	35	37	23	59
13_T_Hum	-35	0	0	23	0	23	47	26	73
Average		0	8	22	0	30	41	24	65
06_T_Hum	-95	0	10	15	0	25	47	23	70
10_T_Hum	-95	0	12	19	0	31	42	22	64
13_T_Hum	-95	0	11	17	0	28	45	23	68
Average		0	11	17	0	28	45	23	67
06_T_Hum	-188	0	8	15	0	23	49	23	72
10_T_Hum	-188	0	8	18	0	26	44	26	70
13_T_Hum	-188	0	7	17	0	24	47	24	71
Average		0	8	17	0	25	47	24	71

206

207 **Table S4.** Hollows - Proportions of sulfur species as calculated by linear combination fittings in living *Sphagnum* and peat profiles
 208 from cores collected in 2012. All values are reported at mol % on a per atom basis. Total oxidized sulfur is the sum of inorganic
 209 sulfate, ester sulfate, sulfone, sulfonate, and sulfoxide. Total reduced sulfur is the sum of thiol, organic monosulfide, thiophene, and
 210 organic disulfide.

Sample ID	Depth to midpoint (cm)	Inorganic Sulfate (%)	Ester Sulfate (%)	Sulfone & Sulfonate (%)	Sulfoxide (%)	Total Oxidized Sulfur (%)	Thiol & Organic Monosulfide & Thiophene (%)	Organic disulfide (%)	Total Reduced Sulfur (%)
06_T_Hol	-5	21	0	18	12	51	40	0	40
07_T_Hol	-5	15	0	18	0	33	36	24	60
10_T_Hol	-5	0	30	0	14	44	35	16	51
13_T_Hol	-5	0	21	16	12	49	43	0	43
17_T_Hol	-5	0	26	13	12	50	42	0	42
21_T_Hol	-5	0	34	0	13	47	31	18	49
Average		6	18	11	10	46	38	10	48
06_T_Hol	-25	0	18	20	0	38	38	20	58
07_T_Hol	-25	0	23	16	0	39	32	22	54
10_T_Hol	-25	0	10	17	0	28	36	30	66
13_T_Hol	-25	0	15	16	0	31	39	23	62
17_T_Hol	-25	0	10	18	0	28	38	27	66
21_T_Hol	-25	0	0	32	12	44	30	21	52
Average		0	13	20	2	35	36	24	59
06_T_Hol	-35	0	11	20	0	31	38	25	62
07_T_Hol	-35	0	15	19	0	33	33	28	61
10_T_Hol	-35	0	15	20	0	36	33	24	57
13_T_Hol	-35	0	11	18	0	28	43	24	66
17_T_Hol	-35	0	0	26	0	26	46	24	70
21_T_Hol	-35	0	14	17	0	31	35	29	64
Average		0	11	20	0	31	38	25	63
06_T_Hol	-95	NA	NA	NA	NA	NA	NA	NA	NA
07_T_Hol	-95	0	12	11	0	23	44	25	69
10_T_Hol	-95	NA	NA	NA	NA	NA	NA	NA	NA
13_T_Hol	-95	0	10	14	0	24	47	22	69
17_T_Hol	-95	8	0	13	0	22	51	24	75
21_T_Hol	-95	0	9	16	0	25	45	24	69
Average		2	8	14	0	24	47	24	71
06_T_Hol	-187.5	0	10	13	0	24	47	20	67
07_T_Hol	-187.5	0	9	13	0	23	49	22	71
10_T_Hol	-187.5	0	10	10	0	21	49	26	75
13_T_Hol	-187.5	0	12	11	0	22	52	21	74
17_T_Hol	-187.5	0	8	13	0	21	52	22	74
21_T_Hol	-187.5	0	8	15	0	23	50	23	73
Average		0	10	13	0	22	50	23	72

211

212 **Table S5.** Mean sulfur speciation in two *Sphagnum* taxa and peatland soils as a function of hummock and hollow topography and
 213 depth. All values are reported at mol % on a per atom basis. Total oxidized sulfur is the sum of inorganic sulfate, ester sulfate, sulfone,
 214 sulfonate, and sulfoxide. Total oxidized sulfur decreases with depth. Total reduced sulfur is the sum of thiol, organic monosulfide,
 215 thiophene, and organic disulfide. Total reduced sulfur increases with depth.

Sample Description	Depth (cm)	Total Sulfur (mM/kg)	Inorganic Sulfate (%)	Ester Sulfate (%)	Sulfone & Sulfonate (%)	Sulfoxide (%)	Total Oxidized Sulfur (%)	Thiol & Organic Monosulfide & Thiophene (%)	Organic disulfide (%)	Total Reduced Sulfur (%)
S. angustifolium / fallax	NA	NA	0	10	33	0	43	36	15	51
S. divinum	NA	NA	16	0	30	0	46	33	13	46
Hollow	-5	48	6	18	11	10	46	38	10	48
	-25	63	0	13	20	2	35	36	24	59
	-35	71	0	11	20	0	31	38	25	63
	-95	59	2	8	14	0	24	47	24	71
	-187.5	69	0	10	13	0	22	50	23	72
Hummock	+25	33	4	13	23	4	43	41	9	49
	+15	39	0	26	13	13	52	37	6	42
	+5	47	0	22	14	4	41	35	19	54
	-5	71	0	13	18	0	31	35	27	62
	-25	68	0	10	22	0	32	39	24	63
	-35	63	0	8	22	0	30	41	24	65
	-95	64	0	11	17	0	28	45	23	67
	-187.5	76	0	8	17	0	25	47	24	71

216

217 **Table S6.** Mean mercury concentrations in peatland soils as a function of hummock and hollow
 218 topography and depth. % MeHg is calculated as $\text{MeHg} \div \text{THg} \times 100$.

Sample Description	Depth (cm)	THg (ng/g)	MeHg (ng/g)	% MeHg
Hollow	-5	74.5	0.8	1.2
Hollow	-25	126.7	2.5	1.9
Hollow	-35	102.6	2.7	2.4
Hollow	-95	33.4	0.7	2.2
Hollow	-187.5	36.8	0.2	0.6
Hummock	+25	42.4	0.3	0.7
Hummock	+15	57.8	0.3	0.5
Hummock	+5	92.9	1.3	1.4
Hummock	-5	140.7	3.6	2.6
Hummock	-25	104.0	1.3	1.2
Hummock	-35	79.0	1.4	1.8
Hummock	-95	35.0	0.5	1.4
Hummock	-187.5	44.2	0.6	1.2

219

220

221 **Table S7.** Spearman’s correlations (rho) between sulfur species and mercury in samples from
 222 hollow (n = 30) and hummock cores (n = 24). Only significant p-values are displayed (p < 0.05).
 223 Black rho values are positive and red rho values are negative. Variables with an “NA” did not
 224 have correlation results that were statistically significant.

Hollow			Hummock		
Total Mercury					
	Rho	P-Value		Rho	P-Value
MeHg (ng/g)	0.726	<0.0001	MeHg (ng/g)	0.793	<0.0001
Ester Sulfate (%)	0.516	<0.01	Ester Sulfate (%)	NA	NA
Sulfone and Sulfonate (%)	0.467	0.01	Sulfone and Sulfonate (%)	NA	NA
Thiol, Monosulfide, Thiophene (%)	-0.751	<0.0001	Thiol, Monosulfide, Thiophene (%)	-0.557	<0.01
Oxidized Total (%)	0.596	<0.001	Oxidized Total (%)	NA	NA
Reduced Total (%)	-0.598	<0.001	Reduced Total (%)	NA	NA

Methylmercury					
	Rho	P-Value		Rho	P-Value
THg (ng/g)	0.726	<0.0001	THg (ng/g)	0.793	<0.0001
Sulfone and Sulfonate (%)	0.634	<0.001	Sulfone and Sulfonate (%)	NA	NA
Thiol, Monosulfide, Thiophene (%)	-0.594	<0.01	Thiol, Monosulfide, Thiophene (%)	-0.506	0.012
Organic Disulfide (%)	NA	NA	Organic Disulfide (%)	0.617	<0.01
Oxidized Total (%)	0.433	0.021	Oxidized Total (%)	NA	NA
Reduced Total (%)	-0.418	0.028	Reduced Total (%)	NA	NA

Percent Methylmercury					
	Rho	P-Value		Rho	P-Value
Total Sulfur (mM/kg)	NA	NA	Total Sulfur (mM/kg)	0.472	0.02
Sulfone and Sulfonate (%)	0.500	<0.01	Sulfone and Sulfonate (%)	NA	NA
Sulfoxide (%)	NA	NA	Sulfoxide (%)	-0.436	0.03
Organic Disulfide (%)	NA	NA	Organic Disulfide (%)	0.670	<0.001

225

226 **Table S8.** Spearman’s correlations between sulfur species and potential methylation rate
 227 constants in the S1 bog from 2012 and 2016, n=36. Variables with an “NA” did not have
 228 correlation results that were statistically significant.

k_m (d ⁻¹) ^a		
	Rho	P-Value
Ester Sulfate (%)	0.555	<0.001
Sulfone/Sulfonate (%)	-0.377	0.023
Total Oxidized (%)	0.377	0.023
Total Reduced (%)	-0.377	0.023

k_d (d ⁻¹) ^b		
	Rho	P-Value
N/A	N/A	N/A

k_{ratio} ^c		
	Rho	P-Value
Ester Sulfate (%)	0.466	<0.01
Thiols / Monosulfides / Thiophenes (%)	-0.374	0.035

a. potential methylation constant

b. potential demethylation constant

c. $K_{ratio} = k_m/k_d*100$

229

230 **Table S9.** Mean potential rate constants in peatland soils as a function of depth. The k_{ratio} is $k_m/$
 231 $k_d * 100$.

Depth (cm)	k_m (d ⁻¹)	k_d (d ⁻¹)	k_{ratio}
0	0.001	2.702	0.021
-5	0.003	2.539	0.123
-10	0.011	1.638	0.653
-15	0.012	1.449	0.815
-20	0.008	1.742	0.464
-25	0.005	2.441	0.214
-30	0.003	1.935	0.151
-40	0.002	2.312	0.081
-50	0.001	3.024	0.041

232

233 **REFERENCES:**

- 234 (1) Haynes, K. M.; Kane, E. S.; Potvin, L.; Lilleskov, E. A.; Kolka, R. K.; Mitchell, C. P. J.
 235 Mobility and Transport of Mercury and Methylmercury in Peat as a Function of Changes
 236 in Water Table Regime and Plant Functional Groups. *Global Biogeochem. Cycles* **2017**,
 237 *31* (2), 233–244. <https://doi.org/10.1002/2016GB005471>.
- 238 (2) Haynes, K. M.; Kane, E. S.; Potvin, L.; Lilleskov, E. A.; Kolka, R. K.; Mitchell, C. P. J.
 239 Gaseous Mercury Fluxes in Peatlands and the Potential Influence of Climate Change.
 240 *Atmos. Environ.* **2017**, *154*, 247–259. <https://doi.org/10.1016/j.atmosenv.2017.01.049>.
- 241 (3) Haynes, K. M.; Kane, E. S.; Potvin, L.; Lilleskov, E. A.; Kolka, R. K.; Mitchell, C. P. J.
 242 Impacts of Experimental Alteration of Water Table Regime and Vascular Plant
 243 Community Composition on Peat Mercury Profiles and Methylmercury Production. *Sci.*
 244 *Total Environ.* **2019**, *682*, 611–622. <https://doi.org/10.1016/j.scitotenv.2019.05.072>.
- 245 (4) Iversen, C. M.; Hansen, P.; Brice, D. J.; Phillips, J. R.; Mcfarlane, K. J.; Hobbie, E. A.;
 246 Kolka, R. K. SPRUCE Peat Physical and Chemical Characteristics from Experimental
 247 Plot Cores , 2012. *Carbon Dioxide Inf. Anal. Center, Oak Ridge Natl. Lab. U.S. Dep.*
 248 *Energy, Oak Ridge, Tennessee, U.S.A.* **2014**.
- 249 (5) Jowsey, P. C. An Improved Peat Sampler. *New Phytol.* **1966**, *65* (2), 245–248.
- 250 (6) Griffiths, N. A.; Sebestyen, S. D. SPRUCE Porewater Chemistry Data for Experimental
 251 Plots Beginning in 2013. *Oak Ridge, TN Carbon Dioxide Inf. Anal. Center, Oak Ridge*
 252 *Natl. Lab. U.S. Dep. Energy* **2016**, 1–15.
- 253 (7) Ravel, B.; Newville, M. ATHENA, ARTEMIS, HEPHAESTUS: Data Analysis for X-Ray
 254 Absorption Spectroscopy Using IFEFFIT. *J. Synchrotron Radiat.* **2005**, *12*, 537–541.
 255 <https://doi.org/10.1107/S0909049505012719>.
- 256 (8) Nicholas, S. L.; Erickson, M. L.; Woodruff, L. G.; Knaeble, A. R.; Marcus, M. A.; Lynch,
 257 J. K.; Toner, B. M. Solid-Phase Arsenic Speciation in Aquifer Sediments: A Micro-X-Ray
 258 Absorption Spectroscopy Approach for Quantifying Trace-Level Speciation. *Geochim.*
 259 *Cosmochim. Acta* **2017**, *211*, 228–255. <https://doi.org/10.1016/j.gca.2017.05.018>.
- 260 (9) 4500-S2- D Methylene Blue Method <http://standardmethods.org/>.
- 261 (10) Tucker, S. *Determination of Sulfide by Flow Injection Analysis Colorimetry. Quik-Chem*
 262 *Method 10-116-29-1D*; Loveland, Co, 2010.
- 263 (11) Grigal, D. .; Kolka, R. K.; Fleck, J. A.; Nater, E. A. Mercury Budget of an Upland-
 264 Peatland. *Biogeochemistry* **2000**, *50*, 95–109.
- 265 (12) Bloom, N. S.; Crecelius, E. A. Determination of Mercury in Seawater at Sub-Nanogram
 266 per Liter Levels. *Mar. Chem.* **1983**, *14*, 49–59.
- 267 (13) Bloom, N. Determination of Picogram Levels of Methylmercury by Aqueous Phase
 268 Ethylation Followed by Cryogenic Gas Chromatography with Cold Vapour Atomic
 269 Fluorescence Detection. *Can. J. Fish. Aquat. Sci.* **1989**, *46*, 1131–1140.

- 270 (14) Mitchell, C. P. J.; Gilmour, C. C. Methylmercury Production in a Chesapeake Bay Salt
271 Marsh. *J. Geophys. Res.* **2008**, *113* (G00C04), 1–14.
272 <https://doi.org/10.1029/2008JG000765>.
- 273 (15) Hintelmann, H.; Evans, R. D. Application of Stable Isotopes in Environmental Tracer
274 Studies - Measurement of Monomethylmercury (CH₃Hg⁺) by Isotope Dilution ICP-MS
275 and Detection of Species Transformation. *Fresenius. J. Anal. Chem.* **1997**, *358*, 378–385.
276 <https://doi.org/10.1007/s002160050433>.
- 277 (16) Hintelmann, H.; Ogrinc, N. Determination of Stable Mercury Isotopes by ICP/MS and
278 Their Application in Environmental Studies. In *Biogeochemistry of Environmentally*
279 *Important Trace Elements*; American Chemical Society: Washington DC, USA, 2003; pp
280 321–338. <https://doi.org/10.1021/bk-2003-0835.ch021>.
- 281 (17) U.S. Environmental Protection Agency. Method 1631, Revision E: Mercury in Water by
282 Oxidation, Purge and Trap, and Cold Vapor Atomic Fluorescence Spectrometry. *EPA*
283 *821-R-96-012* **2002**, 1–46.
- 284 (18) Gionfriddo, C. M.; Wymore, A. M.; Jones, D. S.; Wilpiseski, R. L.; Lynes, M. M.;
285 Christensen, G. A.; Soren, A.; Gilmour, C. C.; Podar, M.; Elias, D. A. An Improved
286 HgcAB Primer Set and Direct High-Throughput Sequencing Expand Hg-Methylator
287 Diversity in Nature. *Front. Microbiol.* **2020**, *11* (541554), 1–23.
288 <https://doi.org/10.3389/fmicb.2020.541554>.
- 289 (19) Gilmour, C. C.; Soren, A. B.; Gionfriddo, C. M.; Podar, M.; Wall, J. D.; Brown, S. D.;
290 Michener, J. K.; Urriza, M. S. G.; Elias, D. A. Pseudodesulfovibrio Mercurii Sp. Nov., a
291 Mercury-Methylating Bacterium Isolated from Sediment. *Int. J. Syst. Evol. Microbiol.*
292 **2021**, *71* (004697), 1–10. <https://doi.org/10.1099/ijsem.0.004697>.
- 293 (20) Gionfriddo, C.; Podar, M.; Gilmour, C.; Pierce, E.; Elias, D. ORNL Compiled Mercury
294 Methylator Database. United States 2019, p N.P. <https://doi.org/10.12769/1569274>.
- 295 (21) Matsen, F. A.; Kodner, R. B.; Armbrust, E. V. Pplacer: Linear Time Maximum-
296 Likelihood and Bayesian Phylogenetic Placement of Sequences onto a Fixed Reference
297 Tree. *BMC Bioinformatics* **2010**, *11* (538), 1–16.
- 298 (22) Verry, E. S.; Bay, R. R.; Boelter, D. H. Establishing the Marcell Experimental Forest:
299 Threads in Time. In *Peatland Biogeochemistry and Watershed Hydrology at the Marcell*
300 *Experimental Forest*; CRC Press: Boca Raton, FL, 2011; pp 1–14.

301